INSTITUT DE FRANCE
Académie des sciences

Comptes Rendus

Physique

Farzad Zangeneh-Nejad, Andrea Alù and Romain Fleury

Topological wave insulators: a review

Volume 21, issue 4-5 (2020), p. 467-499

Published online: 3 November 2020
Issue date: 16 December 2020

https://doi.org/10.5802/crphys.3

Part of Special Issue: Metamaterials 1
Guest editors: Boris Gralak (CNRS, Institut Fresnel, Marseille, France)
and Sébastien Guenneau (UMI2004 Abraham de Moivre, CNRS-Imperial College, London, UK)

Les Comptes Rendus. Physique *sont membres du Centre Mersenne pour l'édition scientifique ouverte*
www.centre-mersenne.org
e-ISSN : 1878-1535

Comptes Rendus
Physique
2020, 21, n° 4-5, p. 467-499
https://doi.org/10.5802/crphys.3

Metamaterials 1 / *Métamatériaux 1*

Topological wave insulators: a review

Isolants topologiques pour les ondes: un état de l'art

Farzad Zangeneh-Nejad [a], Andrea Alù [b] and Romain Fleury [*, a]

[a] Laboratory of Wave Engineering, School of Electrical Engineering, EPFL, Station 11, 1015 Lausanne, Switzerland

[b] Photonics Initiative, Advanced Science Research Center, City University of New York, New York, NY 10031, USA

E-mails: farzad.zangenehnejad@epfl.ch (F. Zangeneh-Nejad), aalu@gc.cuny.edu (A. Alu), romain.fleury@epfl.ch (R. Fleury)

Abstract. Originally discovered in condensed matter systems, topological insulators (TIs) have been ubiquitously extended to various fields of classical wave physics including photonics, phononics, acoustics, mechanics, and microwaves. In the bulk, like any other insulator, electronic TIs exhibit an excessively high resistance to the flow of mobile charges, prohibiting metallic conduction. On their surface, however, they support one-way conductive states with inherent protection against certain types of disorder and defects, defying the common physical wisdom of electronic transport in presence of impurities. When transposed to classical waves, TIs open a wealth of exciting engineering-oriented applications, such as robust routing, lasing, signal processing, switching, etc., with unprecedented robustness against various classes of defects. In this article, we first review the basic concept of topological order applied to classical waves, starting from the simple one-dimensional example of the Su–Schrieffer–Heeger (SSH) model. We then move on to two-dimensional wave TIs, discussing classical wave analogues of Chern, quantum Hall, spin-Hall, Valley-Hall, and Floquet TIs. Finally, we review the most recent developments in the field, including Weyl and nodal semimetals, higher-order topological insulators, and self-induced non-linear topological states.

Résumé. Découverte à l'origine en matière condensée, la notion d'isolant topologique (IT) a été étendue à divers domaines de la physique des ondes classiques, notamment la photonique, la phononique, l'acoustique, la mécanique et les micro-ondes. Dans leur volume, comme tout autre isolant, les IT électroniques présentent une résistance excessivement élevée à l'écoulement des charges, interdisant la conduction métallique. Sur leur surface, cependant, ils présentent des états conducteurs unidirectionnels avec une protection inhérente contre certains types de défauts, au-delà de ce que pouvait laisser présager la physique du transport électronique en présence d'impuretés. Transposés aux ondes classiques, les IT ouvrent une multitude d'applications passionnantes en ingénierie, comme le routage, les lasers, le traitement du signal, les commutations, etc. avec une robustesse sans précédent face à différentes classes de défauts. Dans cet article, nous passons d'abord en revue le concept de base des IT appliqué aux ondes classiques, à partir de l'exemple simple et monodimensionnel du modèle Su–Schrieffer–Heeger (SSH). Nous passons ensuite aux IT à ondes bidimensionnelles, en discutant des analogues pour les ondes classiques des IT de Chern, d'effet Hall quantique, de spin-Hall, de Valley-Hall, et de Floquet. Enfin, nous passons en revue les développements les plus récents dans le domaine, y compris les semi-métaux de Weyl et nodaux, les isolants topologiques d'ordre supérieur et les états topologiques non linéaires auto-induits.

[*] Corresponding author.

ISSN (electronic) : 1878-1535

Keywords. Condensed matter, Photonics, Phononics, Acoustics, Mechanics, Microwaves.

Mots-clés. Matière condensée, Photonique, Phononique, Acoustique, Mécanique, Micro-ondes.

1. Introduction

Phases of matter are conventionally characterized using the so-called Landau's approach [1], classifying them in terms of the symmetries that break spontaneously at phase transitions. In the 1980's, however, the discovery of the so-called quantum Hall effect, the quantum mechanical version of the classical Hall effect, suggested a fresh view on how to distinguish insulating phases [2]. More specifically, this phenomenon, observed in a 2D electron gas subject to an out-of-plane magnetic field, indicated a completely different classification paradigm based on the abstract concept of topology [3], a branch of mathematics concerned with the study of quantities that are preserved under continuous transformations.

Over the past few years, the topological classification of phases of matter has been extensively developed in order to understand the pivotal differences in the physical properties of electronic insulators, allowing for the distinction between ordinary and topological insulators (TIs) [4–6]. In the bulk, like any other ordinary insulator, a TI exhibits an energy band gap separating the valance and conduction bands. However, contrary to normal insulators, TIs support conductive gapless states flowing along their edges. These edge states are characterized by a special non-local integer number, known as a topological invariant or Chern number [7], which guarantees their presence and cannot change unless the insulating phase undergoes a discontinuous transformation that closes the band gap.

The edge modes of topological insulators can exhibit various interesting properties, the most important ones being the robustness of their existence, as well as their resilience to disorder-induced backscattering. Indeed, in order to destroy the presence of the edge states, topology requires that the bandgap is first closed, implying a stringent modification of the bulk properties, impossible with localized edge imperfections or weak disorder. In addition, fermionic topological edge propagation is typically unidirectional or spin-locked, due to symmetry properties that are not broken by most impurity types. In electronics, these features have been established as a cornerstone for the realization of novel devices with a strong immunity against imperfections [8–11]. For instance, new types of spin-resolved electronic devices have recently been proposed that, by taking the advantage of the robustness of TIs, perfectly separate the "read" current path from the "write" one [12, 13]. This leads to not only a better output signal but also an improved reliability of spintronic systems.

Although discovered in quantum condensed matter systems, topological insulators are not intrinsically based on quantum phenomena and, as such, can be also obtained in classical systems. Indeed, the topological properties of insulators boil down to geometrical phase effects [14] that are, in principle, not related to the spatial scale or the physical nature of the system. In a pioneering paper [15], Haldane and Raghu proposed to extend the notion of Chern topological insulators to electromagnetic waves propagating in periodic media comprising magnetically biased ferrites. This sparked a search for classical applications of topological physics, in particular in wave phenomena of various kinds, from electromagnetics and photonics [16–68], to acoustics and phononics [69–100], as well as mechanics [101–122]. Classical wave systems can therefore benefit from a new kind of topologically inherited robustness to defects and disorder. In comparison with their fermionic counterparts, classical topological systems offer a larger control over their space and time properties, representing a particularly relevant platform to design, fabricate and detect all kinds of topological effects that may not be straightforwardly observed in condensed matter systems.

In this paper, we provide a comprehensive overview of recent advances of wave-based classical topological insulators, with an emphasis on the multidisciplinary aspect of this research field, and the important underlying physical concepts. The review is organized as follows: we first discuss the basic consequences of topological order when applied to classical waves, starting from the one-dimensional scenario, which includes the realization of the so-called Su–Schrieffer–Heeger (SSH) model in various wave physical platforms. We then move to two-dimensions, reviewing wave analogues of the quantum Hall and quantum spin Hall phases, as well as other related ideas such as valley-selective waveguiding, and Floquet topological insulators. We next move on to more recent developments of the field including higher-order topological insulators, three-dimensional topological phases in semi-metals, and nonlinear self-induced topological insulators. Finally, the last section reviews some of the most important technology-oriented applications that are actively being pursued for wave-based topological insulators, providing a clear overview of the future directions in this field.

2. Ordinary topological phases

2.1. *One-dimensional wave topological insulators*

One of the simplest forms of topological insulating phase is found in a periodic one-dimensional discrete chain, known as the Su–Schrieffer–Heeger (SSH) chain [123–135], consisting of identical evanescently coupled resonators with alternating coupling coefficients. The unit cell of the SSH tight-binding chain includes two resonators with identical resonance frequency coupled to each other with an intra-cell coupling coefficient K, whereas an extra-cell coupling coefficient J couples adjacent unit cells. When $K = J$, the two dispersion bands of this one-dimensional crystal touch each other at the edge of the Brillouin zone, as a result of band folding. For $K \neq J$, on the other hand, the band structure is gapped, leading to an insulating phase. Depending on whether $K > J$ or $K < J$, this insulating phase can be of trivial or topological nature. In particular, it has been shown that when the value of the extra-cell coupling coefficient is larger than the intra-cell one (i.e. $K < J$), the corresponding insulating phase is of topological nature, supporting mid-gap edge modes at the interface with any trivial insulator. On the contrary, $K > J$ leads to a trivial insulating phase without any edge mode [123]. While both cases ($K > J$ or $K < J$) look similar when only considering the band structure, i.e. the eigenvalues of the tight-bighting Hamiltonian, the topological difference resides in the associated eigenmodes, which shows a band inversion as one goes from the center to the edge of the Brillouin zone. In this one-dimensional case, the topology is defined from the mapping between the Brillouin circle to the space of 2×2 Hermitian Hamiltonian with chiral symmetry (also known as the equator of the Bloch sphere), and is characterized by a winding number [123]. Importantly, this topological invariant is only well defined for chiral symmetric systems, meaning that all of the resonators should have the same resonance frequency. As a consequence, edge modes are robust to any disorder that preserves this symmetry and is not strong enough to close the band gap, which happens at the onset of Anderson localization. Note also that there exist different types of topological phases in one-dimension, which are all symmetry protected, and summarized in the Altland-Zirnbauer classification table for topological phases [136].

Considering the simplicity of the SSH model, this topological system has been implemented in a large variety of classical wave platforms. For instance, in [137] Parto, *et al.*, realized the optical version of the SSH structure making use of 16 identical coupled micro ring resonators fabricated on InGaAsP quantum wells (Figure 1a). By changing the successive distances between the adjacent rings, the strengths of intra-cell and extra-cell coupling coefficients were engineered such that they give rise to a non-trivial topological phase. The inset of Figure 1b illustrates the profile of the corresponding topological mid-gap state, which is pinned to the edge of the array, and exploited for lasing.

The SSH model has also been implemented in acoustics. In [138], Xiao, *et al.* demonstrated the model in a one-dimensional sonic crystal consisting of cylindrical pipes with alternating cross-sectional areas, thereby mimicking the SSH scheme. Figure 1c shows a photograph of the fabricated SSH structure, which consists of two one-dimensional arrays with different topological properties (different winding numbers), connected to each other to form a mid-gap edge state at the phase transition interface. The inset of Figure 1d shows the profile of the edge mode.

The strong localization of the edge mode of the SSH array has been of particular interest for applications such as lasing [137, 139], and sensing [140]. Yet, these kinds of edge modes cannot be used for waveguiding, as they are confined in zero dimensions. In the next part of this section, we move to two dimensions and describe 2D topological insulators whose edge modes are confined in one dimension and can therefore be leveraged for waveguiding and energy transport.

2.2. *Chern wave insulators*

The integer quantum Hall effect (IQHE) provides the first example of a two-dimensional (2D) electronic topological insulator, in which the electrons flow unidirectionally along the edge of a 2D system subject to an out-of-plane external magnetic field [141]. Under these conditions, the Hall conductance takes the quantized values $\sigma_{\mathrm{H}} = Ce^2/h$, in which h is the Plank constant, e is the electron charge, and C is an integer, corresponding to the topological invariant of the system. This quantity, also known as Chern number, is defined as a surface integral over the entire Brillouin zone (BZ), which is a torus in the three dimensional momentum space. The integral is expressed as

$$C = \frac{1}{2\pi}\oint_{\mathrm{BZ}} A(k)\,\mathrm{d}k. \tag{1}$$

The parameter $A(k)$ in (1) is the so-called Berry curvature defined as $A(k) = \nabla_k \times [\langle\psi_n(k)|i\partial_k|\psi_n(k)\rangle]$, in which $\psi_n(k)$ represents the corresponding Bloch state on the nth band, k is the Bloch wave number, and ∂_k and $\nabla_k\times$ are the derivative and curl operators with respect to k, respectively. Since $A(k)$ is an odd function for time-reversal symmetric systems, the Chern number C is zero in the absence of an external magnetic field. Applying a bias odd under time reversal is therefore essential to achieve a non-zero Chern number. Insulating phases with non-trivial topological order exhibit intriguing unidirectional charge transport along their edges. Note that in two dimensions the topology is defined by mapping the Brillouin torus to the entire Bloch sphere. In this picture, a twisted topology corresponds to an obstruction to define the Bloch wave functions over the entire Brillouin zone using a single phase convention [123].

Motivated by the developments of quantum Hall phases in electronic and quantum systems, the classical analogues of such phases were realized shortly thereafter. As mentioned earlier, Chern insulating phases are associated with a broken time reversal symmetry, which can be achieved in the context of microwave engineering using ferromagnetic materials. In [142], Wang *et al.* realized the electromagnetic version of quantum Hall phases based on gyromagnetic microwave materials. This achievement was obtained in a two-dimensional square lattice of ferrite rods, implemented inside a microwave waveguide and biased with an external uniform magnetic field (see Figure 1e). The one-way character of the topological edge mode was studied and demonstrated both in numerical simulations and experiments, as illustrated in Figure 1f.

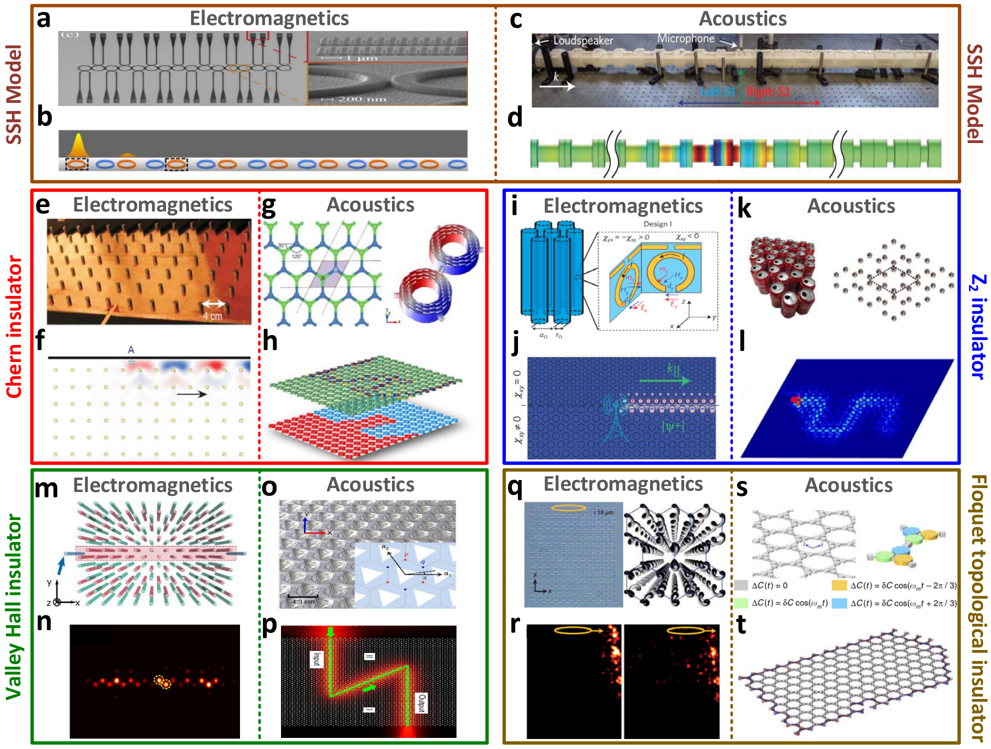

Figure 1. Topological wave insulators. a, b, Realization of a one-dimensional electromagnetic topological insulator (based on the SSH scheme) in an array of coupled micro ring resonators fabricated on InGaAsP quantum wells. c, d, Realization of the SSH model in acoustics based on cylindrical waveguides with alternating cross-sectional areas, tuning the strengths of the coupling coefficients. e, f, Two-dimensional Chern wave insulators were firstly realized in electromagnetics based on a square lattice of magnetically-biased gyromagnetic ferrite rods, implemented inside a microwave waveguide. g, h, Realization of a Chern insulator in acoustics by constructing a hexagonal lattice of sonic ring cavities filled with rotationally biased moving fluids. i, j, Photonic realization of $\mathbb{Z}_2$ wave insulating phases based on a metamaterial with strong bi-anisotropic behavior, providing TE and TM polarized modes with opposite spin-orbit forces. k, l, A strategy to achieve acoustic versions of $\mathbb{Z}_2$ insulators is to expand the primitive unit-cell of a hexagonal lattice to a larger one, and use the corresponding folded degenerate Bloch states as pseudo-spins. m, n, Photonic realization of Valley Hall insulators based on a zigzag edge domain wall of two crystals with opposite on-site potential organizations. o, p, Realization of Valley Hall insulators in a sonic crystal consisting of triangular polymethyl methacrylate rods positioned in a triangular-lattice with opposite rotation angles. q, r, Photonic analogue of Floquet topological insulator, based on a graphene-like lattice of helical waveguides evanescently coupled to each other. The helicity of the waveguides breaks z-reversal symmetry. s, t, Realization of Floquet topological insulator based on a hexagonal lattice of acoustic trimers, with capacitances modulated in time in a rotating fashion.

Just a few years after this work, researchers extended such extraordinary phases to another field of classical wave physics, namely acoustics. This extension, however, required a different trick [143]. In particular, since sound waves do not interact efficiently with magnetic fields, a different strategy was employed to break time-reversal symmetry, namely the use of fluid motion [144]. In 2015, two independent works proposed the use of rotating fluids to realize acoustic analogues of quantum Hall phases [145,146]. Fleury *et al.* proposed an acoustic analogue of magnetically-biased graphene (Figure 1g), based on a honeycomb network of ring cavities filled with rotationally moving fluids [145]. Yang, *et al.* [146] suggested a different approach employing a triangular array of rotating cylinders in a viscous fluid. The corresponding edge modes of such topological phases provide the unique opportunity of reflection-less routing of sound along irregularly shaped pathways, as seen in Figure 1h. Such backscattering-immune classical wave transport has been confirmed in a series of related proposals [147, 148], as well as experimental investigations [149, 150].

2.3. $\mathbb{Z}_2$ *wave insulators*

While Chern insulators require breaking of time-reversal symmetry, there exists another type of topological insulators in two-dimensions that, on the contrary, *preserve* time-reversal symmetry. In electronic condensed matter systems, these insulators are referred to as $\mathbb{Z}_2$ topological insulators, and typically emerge in the presence of spin-orbit coupling, as in the quantum spin-Hall effect [151, 152]. Such phases can be pictured as systems in which two time-reversed copies of a quantum Hall phase with opposite Chern numbers coexist without coupling. One of the copies corresponds to electrons with positive spins, and its time-reversed version to electrons with negative spins. As a consequence, two topological edge modes exist that propagate in opposite directions, carrying electrons with different spins. In presence of time-reversal symmetry, Kramers theorem prevents any interaction between the two spin species, which cannot backscatter at non-magnetic defects. Since they do not require time-reversal symmetry breaking, $\mathbb{Z}_2$ topological insulators may appear easier to realize than the Chern class in electronic systems. Yet, realization of these phases in classical systems is not quite straightforward for two principal reasons. First, photons (and also phonons), associated with electromagnetic (or sound) waves, are spin-less particles. Second, they are bosons, for which the time-reversal operator $\mathcal{T}_b$ squares to $+1$, and not to -1, as for electrons, which are fermions ($\mathcal{T}_f^2 = -1$). Interestingly, the relation $\mathcal{T}_f^2 = -1$ is essential for Kramers theorem to hold, guaranteeing truly independent spin subspaces. In order to solve these issues, one must construct a pseudo-spin degree of freedom and "augment" bosonic time-reversal with another symmetry operation $\mathcal{C}$ such that $(\mathcal{C}\mathcal{T}_b)^2 = -1$, enforcing Kramers degeneracy when both $\mathcal{C}$ and $\mathcal{T}_b$ are preserved [153–186]. Note that this procedure potentially makes the classical version of a $\mathbb{Z}_2$ topological phase less robust than its electronic counterpart, since not only $\mathcal{T}_b$ breaking defects induces backscattering for the topological edge modes, but also defects that break $\mathcal{C}$.

For electromagnetic waves, described by Maxwell equations, spin can be emulated by leveraging electromagnetic duality as an additional symmetry $\mathcal{C}$, by enforcing $\varepsilon = \mu$. This assumption indeed restores the duality of Maxwell's equations, creating two degenerate, time-reversed (pseudo)spins. By properly introducing some bi-anisotropy (coupling the TE and TM components of the field), the two spins of such a system can undergo opposite interaction terms emulating spin-orbit coupling. This leads to the realization of an electromagnetic analogue of the quantum spin Hall effect, based on the combination of duality and time-reversal symmetry. Employing this scheme, in [187] Khanikaev *et al.* proposed the photonic analogue of the quantum spin Hall effect in a hexagonal lattice of a spin-degenerate dual metamaterial, composed of split ring resonators with strong bianisotropic behavior (Figure 1i). The inset of Figure 1j represents the profile of one (spin up) of the corresponding edge modes. Defects in the form of sharp turns that do not couple the two polarizations do not break duality nor time-reversal symmetry, hence they do not reflect the spin-locked topological edge modes that can seamlessly be routed along an irregularly shaped topological interface. Note that the duality condition $\varepsilon = \mu$ is hard to achieve as dispersive effects might make it difficult to guarantee this condition over a broad frequency range. Nevertheless, it can be enforced with very good approximation over a couple of crystal bands, which is more than sufficient for observing exceptionally robust edge wave transport along bent paths. A similar idea has been implemented for Lamb waves over a structured plate based on accidental degeneracy between two Lamb modes with distinct polarizations [188]. Finally, the extension of these concepts to continuous electromagnetic media satisfying a generalized form of symmetry, $\mathscr{PTD}$ symmetry, has been successfully conducted by a series of paper by Silveirinha [189, 190]. These photonic systems have similar properties as those based on duality.

In fluid acoustics, the explained strategy to achieve quantum spin Hall phases is not readily functional due to the absence of a polarization degree of freedom. An alternative strategy to emulate acoustic pseudospin is to exploit the symmetry of a crystal lattice, in which case $\mathscr{C}$ is some sort of crystalline symmetry operation. Such a scheme, based on six-fold rotational symmetry, was initially proposed by Wu and Hu in 2015 in a triangular lattice of hexagonal resonators [191], and implemented in a variety of platforms including microwaves [192], photonics [193–197], elastic [198–201] and acoustics [202–205]. Figure 1k and 1l show an example [205] that employed this strategy to induce a deeply subwavelength acoustic topological edge mode in a subwavelength sonic crystal made of Helmholtz resonators (simple soda cans) arranged in a modified hexagonal-like lattice. The unit cell of the crystal is shown in the inset of Figure 1k. Figure 1l illustrates how the edge mode of such a crystal propagates with good transmission along a path involving sharp turns. Note that all symmetry-based strategies for emulating pseudo-spins only allow for an approximate realization of Kramers degeneracy, which only holds at the high-symmetry points of the Brillouin zone (Γ point in the case of six-fold rotational symmetry). Thus, the quantum spin-Hall Hamiltonian can only be emulated “locally” around this degenerate point, as may be proven by performing a first order $k \cdot p$ approximation of the Hamiltonian around the point [191]. However, pushing the $k \cdot p$ analysis beyond first order reveals that Kramers degeneracy is quickly broken away from the high symmetry point, on the same band. Direct use of topological quantum chemistry concepts [206] has confirmed the impossibility of rigorously defining a global $\mathbb{Z}_2$ topological invariant on the entire band structure of these systems. Rigorous quantitative statistical analysis of the edge mode robustness against different kinds of defects [207] is also consistent with an incomplete, or approximate, level of topological protection. Nevertheless, designs based on exploiting crystalline symmetries work very well in practice, and they allow easy and direct exploitation of topological ideas based on lattice symmetries regardless of the physical platform, still leading to relatively large robustness to backscattering.

2.4. *Valley Hall wave insulators*

In a hexagonal lattice in which the Dirac degeneracy has been lifted by breaking inversion symmetry, modes belonging to the K and K' valleys, which are obviously time-reversed images of each other, also carry some form of chirality or pseudospin [208–245]. Locally, these time reversed pairs, which correspond to valleys created by opening time-reversed Dirac cones, carry an opposite Berry flux. Since inversion also changes the K valley into the K' one, one can construct two crystals, inversion images of each other, with valleys having opposite Berry fluxes oriented along a given direction. Then, interfacing these two crystals along this direction amounts to requiring an abrupt sign change of the Berry flux, which requires the band gap to close at the interface, supporting the necessary presence of an edge mode. Similar to the schemes based on six-fold rotational symmetries, it is not possible to define a global topological invariant over the full Brillouin zone, and this type of edge modes is not globally topological. However, it remains exceptionally robust to Valley-preserving defects, like Z shaped turns. In [246], Noh, *et al.* leveraged the valley degree of freedom to realize photonic analogues of the Valley Hall effect in a two-dimensional honeycomb lattice of optical waveguides, shown in Figure 1m. The red and green waveguides in the figure possess different refractive indices, corresponding to two different on-site potentials that allow inversion symmetry breaking. The valley edge modes were obtained along a zigzag edge domain between two crystals with opposite on-site potential configurations (referred to as AB and BA). Under this condition, the edge modes cross the band gaps formed at the proximity of high-symmetric corners of the Brillouin zone. The inset of Figure 1n illustrates the profile of one of the corresponding edge modes.

Interestingly, the valley Hall waveguiding scheme also works in other types of lattices, when some form of operation that flips the sign of the Berry curvature is used. For instance, topological valley Hall phases were realized in acoustic systems based on symmetry-breaking rotations of the crystal constituents. In [247], Lu *et al.* built a sonic valley Hall waveguide with a sonic crystal consisting of triangular polymethyl methacrylate rods (Figure 1o) positioned in a triangular lattice with a rotation angle α with respect to the vector $\boldsymbol{a_1}$. When $\alpha = n\pi/3$, the crystal supports two-folded Dirac cones at the edge of the Brillouin zone. These degeneracies are lifted for other rotation angles, opening a frequency band gap. By connecting two different domain walls with opposite rotation angles of $\alpha = 10°$ and $\alpha = -10°$ corresponding to opposite Berry fluxes, a pair of valley chiral edge states, counterpropagating at the interface, can be realized. Such edge modes can be utilized for guiding of sound along an irregularly shaped zigzag path (Figure 1p). This method is transposable to other wave platforms, including highly dispersive ones, such as gravity-capillary waves at the surface of liquids [248].

2.5. *Floquet topological insulators*

Another conceptually distinct route to achieve electronic topological phases without the need for an external magnetic field is to apply a time-periodic modulation in the electron potential energy or hopping rate [249–251]. In the field of semiconductor physics, it was firstly shown [252] that, by irradiating a trivial semiconductor quantum Well with a time periodic microwave wave, a new kind of topological phase transition can be achieved. Such topological phases, dubbed as Floquet topological insulators, support helical edge modes in their quasi-energy spectral gaps.

Parallel to the developments of Floquet topological insulators in condensed matter systems, these concepts were extended to classical systems [253–267]. In [268], Rechtsman, *et al.*, demonstrated the photonic analogue of a Floquet topological insulator, based on a graphene-like lattice of helical waveguides evanescently coupled to each other, as seen in Figure 1q. The dynamics of beam diffraction through such a lattice is described by the Schrödinger equation, where the distance of propagation takes the role of time. The helicity of the waveguides breaks z-reversal symmetry, effectively emulating time-Floquet modulation, in which the coordinate space z takes the role of time. Within the framework of this mapping, the quasi-band structure of the crystal becomes identical to the one of a Floquet topological insulator, supporting one-way edge states that are protected from scattering at the lattice corners. Shown in Figure 1r is the profile of such edge modes when a beam excites the array from its top edge.

Time-Floquet topological insulators have also been proposed in acoustics. In [269], Fleury *et al.* demonstrated a time-Floquet topological insulator based on a hexagonal lattice of acoustic trimers, whose acoustic properties were periodically modulated in time in a rotating fashion, with uniform handedness throughout the lattice (Figure 1s). Figure 1t shows the profile of one of the corresponding edge states, flowing across the boundary of a finite piece of such a crystal. Compared to acoustic quantum Hall phases discussed in Figure 1g and h, such kinds of topological states are potentially more practical as they do not rely on moving background fluids.

It is also worth mentioning at this point that a one-to-one correspondence between time-Floquet systems and unitary scattering networks can be made, where the unitary network scattering matrix takes the role of the Floquet time-evolution operator over a period [270, 271]. This has allowed an easier experimental exploration of different Floquet topological phases (Chern or anomalous [272]), in both photonics and acoustics [273–275].

3. Topological semimetals

In 2D periodic systems, the topological phases usually stem from point degeneracies in the band structure, which are known as Dirac cones. By properly tuning the system parameters, the degenerate points can be lifted, and bandgaps can be opened, leading to different topologies. In three dimensions, possible band degeneracies are line nodes [276–282], Weyl points [283–303], or 3D Dirac points [304–311]. Weyl points are particularly interesting as they behave as sources of Berry flux, carrying a Chern number of ± 1, which manifests itself as topological surface states along any surface interface enclosing a non-vanishing number of Weyl charges [16].

Following the discovery of Weyl and nodal semimetals in the field of semiconductor physics [284], Lu *et al.* theoretically realized both line nodes and Weyl points in a gyroid photonic crystal made from germanium high-index glasses [312]. Shown in Figure 2a is the real space unit cell of the 3D periodic structure. By applying proper symmetry-breaking perturbations to the unit-cell of such structure, a nodal line degeneracy was realized. This is accomplished by replacing part of the gyroids with air spheres, as seen in the inset of Figure 2a. Figure 2b represents the 3D band structure of the crystal cut at (101) plane. A closed line degeneracy around the Γ point is observed in the band structure of the crystal. Note that the area enclosed by this line degeneracy can be controlled by the strength of the applied perturbation, that is, the radius of the air-sphere.

The unit cell of the crystal in Figure 2a respects parity-time (PT) symmetry. A possible approach to achieve Weyl point degeneracies is to break the PT symmetry of the unit cell. In fact, it is known that a line node degeneracy creates either a frequency band gap or a set of paired Weyl points upon breaking PT symmetry. The PT symmetry of the double gyroid crystal can be broken by, for example, removing one of the air spheres of the two gyroids. By doing so, the line node degeneracy splits into four Weyl degenerate points along ΓN and ΓH directions, as observed in the band structure of Figure 2c.

Weyl and nodal semimetals have also been realized in acoustic systems. In [313], Xiao, *et al.* theoretically discussed the possibility to achieve Weyl and nodal semimetals in a lattice made of coupled sonic resonators and waveguides, described by a tight-binding model involving chiral interlayer couplings. A few years later, phononic Weyl phases were experimentally demonstrated [314] in a chiral phononic crystal, fabricated using layer-stacking technique. The insets of Figure 1d represent the corresponding 3D structure, consisting of stacked layers of air-filled hollow waveguides, connected to each other via spiral hollow channels. Such a structure supports two pairs of Weyl points at $k_z = 0$ and $k_z = \pi/a$. Shown in Figure 2d is the measured band structure of the crystal for $k_z = 0$, from which the existence of Weyl points at the high-symmetry point K is apparent. The inset of Figure 2e shows the Fermi arcs of the corresponding surface states.

Despite the fact that topological semi-metallic phases have successfully been demonstrated in photonic and phononic systems, the realization of such phases is often challenging due to their 3D structure. Based on the notion of synthetic dimension, in [315] Lin, *et al.* explored Weyl physics in a planar 2D geometry, consisting of on-chip ring resonators with dynamic modulation of the refractive index, as sketched in Figure 2g. Each resonator supports a set of discrete modes, whose resonance frequencies are equally spaced. These discrete resonance modes can therefore be pictured as a periodic lattice in the synthetic frequency dimension. Together with the real dimensionality of the crystal, this third, synthetic frequency dimension

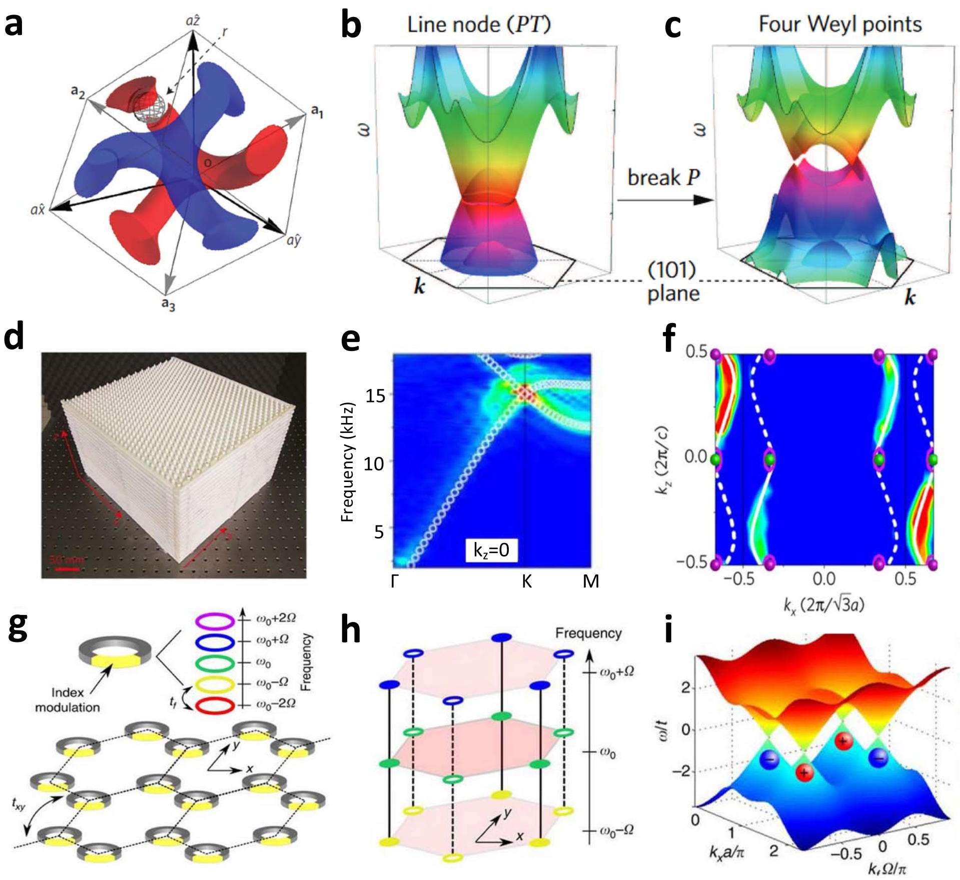

Figure 2. Classical wave Weyl semimetals. a, Realization of electromagnetic analogues of topological semimetals based on a crystal with the real-space unit cell shown in the panel, consisting of two inversion-symmetric gyroids made of germanium high-index glasses. b, Band structure of the corresponding nodal semi metallic phase. c, By breaking the spatial inversion symmetry of the unit cell, the line node degeneracy splits into four distinct Weyl points. d, Realization of acoustic topological semimetals in a chiral phononic crystal fabricated using a layer-stacking strategy. The structure consists of stacked layers of air-filled hollow waveguides, connected to each other via spiral hollow channels. e, Band structure of the crystal shown in panel f, exhibiting Weyl degeneracy at K point. f, Fermi arc surface of the corresponding topological states. g, Exploring Weyl physics in a planar 2D geometry, consisting of on-chip ring resonators with dynamic modulation of refractive indices. h, The discrete resonance modes can be pictured as a periodic lattice in the synthetic frequency dimension. i, Band structure of the crystal in the 3D synthetic dimension, exhibiting four Weyl points.

forms a three-dimensional space (Figure 2h). By modulating the refractive indices of the ring resonators properly, one can then appropriately couple these modes to each other so as to achieve Weyl point degeneracies in the 3D synthetic space formed by the two spatial dimensions and the frequency axis. The inset of Figure 2i shows the corresponding Weyl points and their charges.

4. Higher-order topological insulators

All the topological phases discussed thus far obey the so-called bulk boundary correspondence principle [316, 317] in codimension 1, stating that a d-dimensional topological insulator with Chern number C, hosts a number C of $d-1$ dimensional boundary states, when interfaced with a trivial insulator. Recently, a new class of topological phases has been proposed, which obeys another form of bulk-boundary correspondence. These topological phases of matter, called higher-order topological insulators, exhibit gapped boundaries that are themselves topological phases in a lower dimension. A d-dimensional higher order topological insulator (of order n) supports $d-n$ dimensional gapless boundary states. For instance, a two-dimensional second order topological insulator supports zero dimensional (0D) topological corner states that, as their name suggests, are localized not only at the edges, but also at the "edges of edges", i.e., at the corners of the insulator [318–325].

In [326], Benalcazar, *et al.* theoretically introduced the concept of higher-order topological insulators, based on a C_4 symmetric square lattice crystal with detuned hopping terms and two non-commuting reflection symmetries, leading to an insulating phase with quantized Wannier centers and a quadrupole bulk polarization. Both ordinary 1D edge states and higher-order 0D corner states were simultaneously realized in this lattice. Following this theoretical proposal, higher-order topological states were experimentally observed in various fields. For instance, in electronics a topological circuit was introduced in [327], realizing 0D corner modes. The circuit, shown in Figure 3a, consists of LC tanks coupled to each other via coupling capacitances. The connectivity of the circuit elements guarantees the required C_4 rotational symmetry of the Hamiltonian, as well as the two non-commuting reflection symmetries with respect to x and y directions. Hence, the circuit can indeed be pictured as a second-order topological phase supporting gap-less corner states. The corner mode of the circuit shows itself as a topological boundary resonance in the corner impedance profile of the circuit, as seen in Figure 3c.

At microwaves, higher-order topological insulators have been implemented [328] in a square lattice with unit cell composed of four identical resonators, implemented using H-shaped microstrip transmission lines (Figure 3d). Adjacent cells were connected to each other via transmission lines with proper lengths. Figure 3e shows the measured spectrum of the absorption coefficient, exhibiting in-gap resonances corresponding to the corner state. The inset of Figure 3f shows the spatial distribution of absorptance, summed over the shaded bands. It is observed that the corner states are indeed localized at the four corners of the crystal.

Higher-order topological insulators have also been transferred to the realm of acoustics. In [329, 330], Xue *et al.*, and Ni *et al.*, independently demonstrated a second-order topological insulator in an acoustic metamaterial, based on a breathing Kagome lattice with non-trivial bulk polarization. The corresponding Kagome lattice is shown in Figure 3g, consisting of coupled acoustic air-filled cylindrical resonators with metal walls. When the extra-cell couplings become higher than the intra-cell ones, the lattice crystal under study becomes topological (of second-order character). Figure 3h represents the spectrum of normalized density of states obtained from the measurements of acoustic energy stored in the bulk (yellow), at the edges (red) and corners (blue) of the crystal. Figure 3i shows the profile of the corresponding corner state integrated over the corresponding frequency region. Such 0D states hold great promise for controlling and trapping waves at specific points in a robust fashion, which is relevant in a variety of applications such as energy harvesting, lasing, sensing, and enhanced wave-matter interactions.

In the context of mechanical topological insulators, the in-gap corner states have also been realized and experimentally observed on a structured elastic plate [331]. The realization is based on a perturbative mechanical metamaterial shown in Figure 3j, consisting of coupled plates of single-crystal silicon. The thin beams between the nearest neighboring plates controls the sign

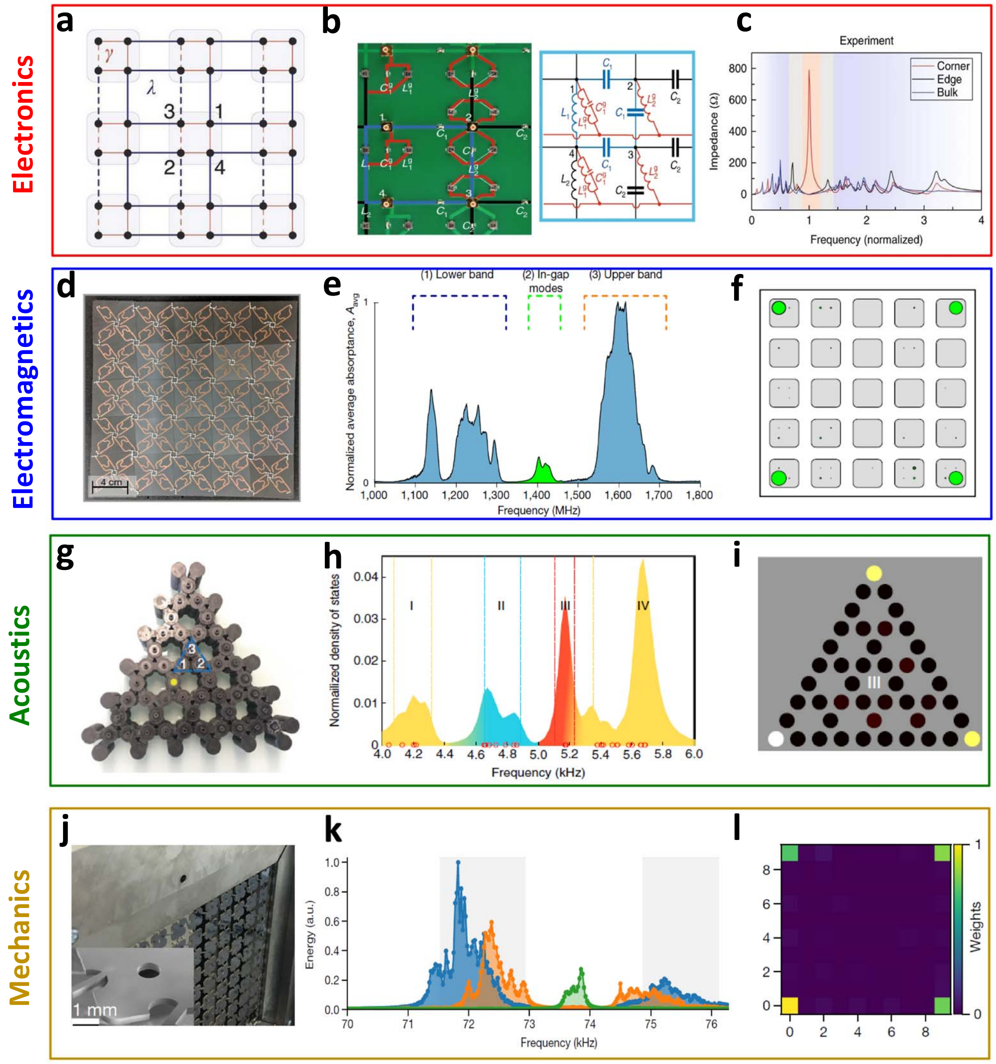

Figure 3. Higher-order classical topological insulators. a, Tight binding lattice realizing topological corner modes. b, A circuit design realizing corner modes circuit, consisting of *LC* tanks coupled to each other via some coupling capacitances. c, Corner impedance profile of the circuit, exhibiting a dominant resonance peak associated with the topological corner mode. d, Realization of higher order topological states in microwaves, based on a square crystal of four identical resonators implemented using H-shaped micro strip transmission lines. e, The measured spectrum of the absorption coefficient, exhibiting in-gap resonances corresponding to the corner state. f, Spatial distribution of absorptance, summed over the shaded bands. g, Acoustic higher order topological insulators based on a Kagome lattice with a non-trivial bulk polarization. The structure consists of coupled acoustic air-filled cylindrical resonators with metal walls. h, Spectrum of normalized density of states obtained from measuring acoustic power at the bulk (yellow), edge (red) and corner (blue) of the crystal. i, Profile of the corresponding corner state. j, Realization of an elastic second order mechanical topological insulator based on a perturbative mechanical metamaterials consisting coupled plates of single-crystal silicon. k, Spectrum of the bulk (blue), edge (orange) and corner (green) modes. l, Profile of the corner mode of the structure at its resonance frequency.

and amplitude of the corresponding coupling coefficients. Figure 3k shows the spectrum of bulk (blue), edge (orange), and corner (green) states, when the structure is excited with an ultrasound air-transducer. Figure 3l depicts the profile of corner states, demonstrating their confinement to the corners of the crystal. Other realizations of higher-order TIs have been reported in [332–346].

5. Nonlinear topological insulators

All topological phases discussed thus far are based on linear structures. The presumption of linearity, albeit crucial to define a band structure, can however imply stringent geometrical conditions. For instance, in order to realize spin Hall phases in the acoustic lattice crystal discussed in Figure 1g and h, the extra cell coupling between resonators are necessarily required to be larger than the intra-cell ones. Amplitude-dependent nonlinear phenomena [347–352], however, can be utilized to achieve the same kind of topological phases without this special condition. In [353], Hadad *et al.* investigated a one-dimensional nonlinear topological system based on a SSH toy model with nonlinear staggered potentials (Figure 4a). Each unit cell of the SSH array consisted of two atoms with the same on-site potentials. These atoms were connected to each other via linear intra-cell coupling κ_0. The nearest-neighboring cells were connected to each other with amplitude-dependent nonlinear extra-cell coupling coefficients of the form $\vartheta_n = \vartheta_0 + \alpha(|a_n^{(1)}|^2 + |a_n^{(2)}|^2)$, in which $\vartheta_0 < \kappa_0$ is a constant, and α is a Kerr coefficient. Under these assumptions, and assuming weak nonlinearity, the dynamics of the system can be expressed with a tight-binding Hamiltonian of the form $H = \cos(k_B a)[\kappa_0 - (\vartheta_0 + \alpha I(|a_0^{(1)}|^2 + |a_0^{(2)}|^2))]\sigma_x + \sin(k_B a)[(\vartheta_0 + \alpha I(|a_0^{(1)}|^2 + |a_0^{(2)}|^2))]\sigma_y$, in which σ_x are σ_y are Pauli matrices. Note that, in contrast to the linear case, the Hamiltonian H depends on the eigenstates of the system. Hence, in principle, its eigenvalues should be calculated in an iterative manner. Since $\vartheta_0 < \kappa_0$, the Hamiltonian H corresponds to a trivial insulator at low excitation intensities ($I \to 0$), exhibiting a frequency band gap that is topologically trivial. The enhancement of the field amplitude, however, effectively increases the extracell couplings. At some threshold intensity I_{th}, the strengths of ϑ_n and κ_0 become equal, which closes the band gap and results in a topological phases transition. By increasing the excitation intensity further, the strength of extra-cell couplings becomes larger than that of the intra-cell ones, opening a band gap in the band structure of the crystal with a nontrivial topological order (Figure 4b). Interestingly, these predictions based on assumptions of periodicity for the infinite non-linear lattice correctly predict the behavior of edge modes when the non-linear system is truncated to a finite size. Figure 4c shows the evolution of the mode profile of the mid-gap state versus intensity, illustrating the transition from bulk to exponentially decaying edge modes. Note that, as opposed to their linear counterparts, these nonlinear topological edge states decay to a plateau of non-zero amplitude, highlighting the local nature of the associated band gaps [353]. Essentially, as the intensity of the mode decays away from the edge, locally the gap becomes narrower, and asymptotically tends to close, yielding the plateau profile that extends into the lattice.

Such kinds of topological phases with nonlinear staggered potentials have been implemented in a circuit [354], composed of *LC* tanks connected to each other with linear capacitances (intra-cell dynamics) and nonlinear varactor diodes (extra-cell dynamics), as seen in Figure 4d. Shown in Figure 4e is the spectrum of the input admittance of the circuit at high power intensity, corresponding to a non-trivial topological phase. As observed, the spectrum exhibits a dominant resonance peak, which corresponds to the self-induced topological corner state. Figure 4f exhibits the voltage distribution of the circuit at the resonance frequency of the corner mode.

Not only does the nonlinear phenomenon allow one to achieve self-induced topological phases, but it also establishes an ideal platform for dynamically tuning the spectral and localization characteristics of the edge modes. In [355], Dobrykh, *et al.* demonstrated such a striking

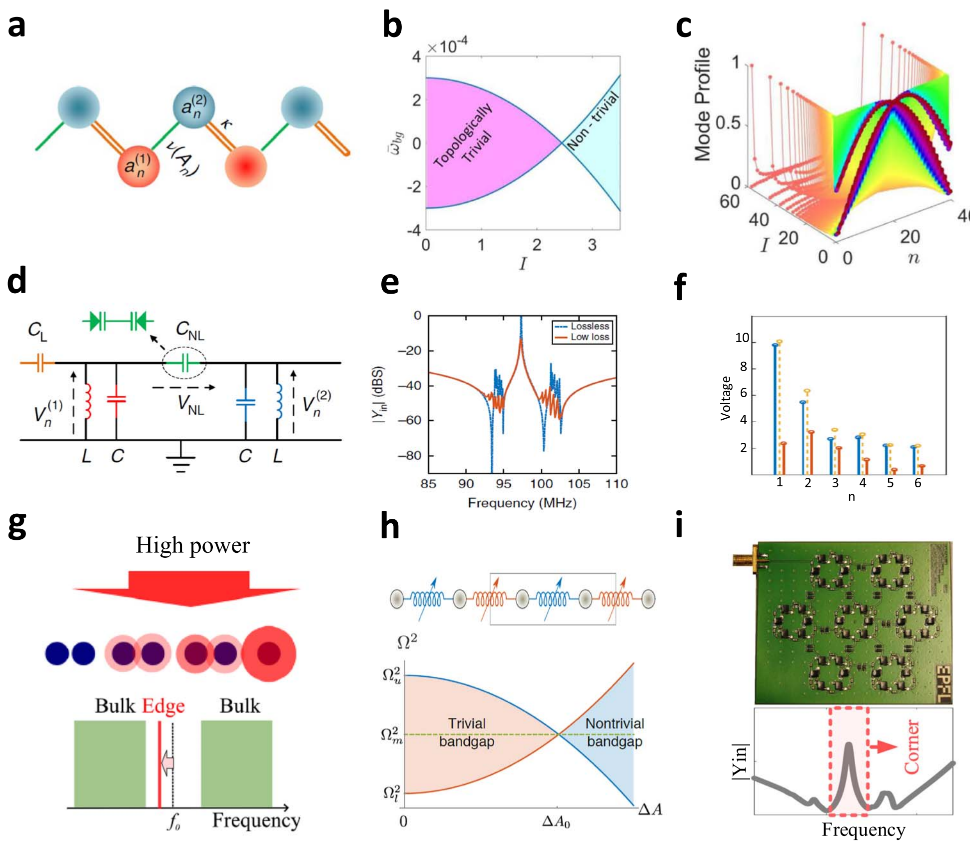

Figure 4. Nonlinear self-induced classical topological insulators. a, A one-dimensional nonlinear topological system, based on a SSH toy model with alternating linear and nonlinear staggered potentials. b, Evolution of the band gap of the SSH array versus the excitation intensity. At low excitation intensities, the SSH array is topologically trivial, with its extra-cell couplings being smaller than the intra-cell ones. Enhancing the excitation intensity, however, closes the band gap of the crystal and re-opens it as topological. c, Evolution of the mode profile of the mid-gap state versus intensity. d, Implementation of the nonlinear topological insulator discussed in Figure 4a, based on a circuit lattice composed of *LC* tanks connected to each other via linear capacitances (intra-cell dynamics) and nonlinear varactor diodes (extra-cell dynamics). e, Spectrum of the input admittance of the circuit at high power intensity. The spectrum exhibits a dominant resonance peak, which corresponds to the self-induced topological corner state. f, Voltage distribution of the circuit at the resonance frequency of the corner mode. g, Enhancing the excitation intensity allows one to tune the spectral characteristics of the topological edge mode of a one-dimensional photonic crystal. h, Self-induced topological phase transition in a SSH array consisting of masses connected to each other with two types of alternating nonlinear springs, dubbed as "stiffening" (orange) and "softening" (blue). i, Self-induced second order topological insulator, based on a circuit lattice of *LC* tanks, connected to each other with alternating linear and nonlinear capacitors. The circuit supports zero-dimensional topological corner modes, manifesting themselves as a dominant resonance peak in the corner input admittance spectrum of the circuit (bottom panel).

possibility for a one-dimensional SSH array of coupled nonlinear photonic resonators. The array is designed to be of topological nature in the linear regime, corresponding to low excitation intensity. Hence it supports an edge mode, protected by chiral symmetry, at its boundary. When the excitation intensity is enhanced, the spectral line shape of the edge modes shifts towards the bulk modes as observed in Figure 4g, top. This shift reduces the localization of the edge modes as seen in the bottom panel of the figure. These observations demonstrate how the nonlinear phenomenon enables dynamic reconfiguration of the spectral characteristics of the supported topological edge modes.

The nonlinear phenomenon has also been studied in phononic systems to achieve self-induced topological transitions. In [356], Chaunsali and Theocharis demonstrated such kind of transitions in a SSH array consisting of masses connected to each other with two types of alternating nonlinear springs (Figure 4h), namely "stiffening" and "softening" types. As mentioned earlier, such system can go through a topological phase transition by enhancing the excitation intensity and invoking the nonlinear dynamics. The bottom panel of Figure 4h illustrates the evolution of the band gap of the SSH structure versus the excitation intensity, indicating the topological phase transition induced by nonlinearity.

Finally, we remark that nonlinear phenomena have also been applied to realize self-assembled higher-order topological insulators. In [357], it was shown how the nonlinear phenomenon can be leveraged to achieve self-induced topological corner states. Unlike the linear case, the spectral properties of such 0D topological modes can be tuned by changing the excitation intensity, enabling dynamic reconfigurability. The inset of Figure 4i (top) shows the realization of such topological phases in a modified hexagonal lattice of *LC* tanks, connected to each other via alternating linear and nonlinear coupling capacitors. The circuit is designed to be in the trivial phase when it is excited at a low excitation intensity. Upon enhancing the excitation power, however, the circuit becomes topological (of second-order character), supporting zero-dimensional corner states. Such topological states manifest themselves as a resonance peak in the corner admittance spectrum of the circuit, as seen in Figure 4i (bottom panel).

6. Applications

In the previous sections we have discussed how the field of topological insulators has provided a rich platform to manipulate waves in a variety of platforms, and to implement topological phases of matter in classical wave physics. However, the impact of this area of research has been rapidly expanding in the realm of practical applications of these concepts, as we detail in this section, in which we discuss the most important recently proposed technology-oriented applications of topological wave insulators.

6.1. *Robust waveguiding*

An important application of classical topological insulators is robust guiding of energy over arbitrary paths [357–380]. An ordinary waveguide exhibits a bi-directional type of dispersion. On the contrary, the gapless edge states of Chern wave insulators possess a frequency dispersion with only positive (or negative) slope (or group velocity). Consequently, waves (light or sound) cannot couple to any backward state when it reaches an imperfection, and does not backscatter. Suppose that a perfectly conducting obstacle is placed on the way of the electromagnetic wave propagating along the edge of the topological system discussed in Figure 1e. While this normally induces strong reflection in any ordinary waveguide, the topological insulator lets the electromagnetic energy flow around the PEC with perfect transmission (Figure 5a). Such fascinating property has also been proposed in acoustics for reflection-less guiding of sound waves. Figure 5b shows how

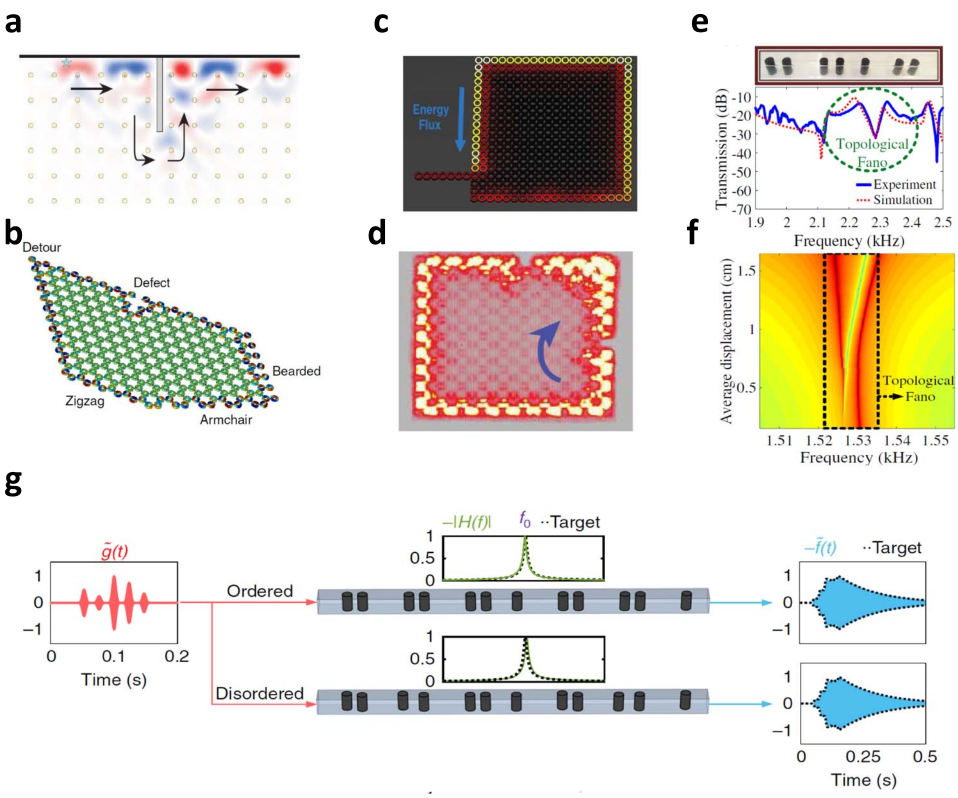

Figure 5. Applications of classical wave topological insulators. a, In contrast to any ordinary type of waveguide, the edge mode of the topological insulator discussed in Figure 1a smoothly flows around a PEC obstacle without backscattering, enabling robust guiding of electromagnetic energy. b, Reflection-less guiding of sound waves using the topological insulator discussed in Figure 1c. Despite the presence of several types of defects on the way of the edge mode, it flows along the perimeter of the crystal with almost perfect transmission. c, Theoretical realization of the lasing action from the edge mode of a topological insulator, based on an aperiodic topological array of micro ring resonators. d, Experimental demonstration of the lasing action. The lasing mode shows strong robustness to disorder. e, By inducing two topological subspaces of even and odd modes in a SSH array of cylinders arranged inside a monomode acoustic waveguide (top panel), a new class of Fano resonances, namely topological Fano resonances, is obtained (bottom panel). f, Evolution of the spectral line shape of the topological Fano resonance versus disorder strength. g, Topological analog signal processing based on the mid-gap state of a SSH array, built from cylindrical rods arranged inside an acoustic waveguide. Upon exciting the mid-gap state, such a system performs time domain differential equation solving (top signal path), with a strong immunity against imperfection (bottom signal path).

the edge mode of the acoustic topological insulator discussed in Figure 1g ideally travels along an interface involving various types of defects and detours. This is in stark contrast to ordinary acoustic waveguides in which two subsequent defects always create Fabry–Pérot interferences and, more generally, impedance matching issues. These unusual properties have been proposed to realize compact delay lines [381].

6.2. *Lasing*

Another promising application of topological insulators is single-mode robust lasing [382–389]. In [389], Harari, *et al.*, theoretically proposed to achieve the lasing action from the edge modes of a topological insulator. The realization was based on an aperiodic topological array of micro-ring resonators, which was one of the basic platforms explored for achieving photonic topological insulators [390, 391]. The aperiodic nature of such structure creates an artificial gauge field, allowing one to have edge states analogues to quantum Hall phases without the presence of any external magnetic field. By providing gain to the resonator cavities located on the perimeter of the crystal, the lasing action from such a configuration was demonstrated, as seen in Figure 5b, and demonstrated to be robust to spin-preserving defects.

Based on these theoretical findings, in [392], Bandres *et al.* experimentally verified the lasing action from such kind of a system. Figure 5c represents the lasing from such a topological system. Remarkably and consistent with the topological nature of the structure, the lasing mode and its slope efficiency shows a strong immunity against disorder. We note that the edge modes of this topological lasing systems are time-reversal symmetry preserved and, as such, are not truly unidirectional. Yet, there are proposals [383] on the realization of topological lasers with a broken time-reversal symmetry, enabling truly unidirectional and non-reciprocal lasing action at telecommunication wavelength.

6.3. *Fano resonances*

Fano resonances are caused by the interference between a sharp resonance state (the dark state) with a wider-band one (bright state). Such exotic kind of resonances, which are characterized by an asymmetric and ultra-sharp spectral line shape, have found a large variety of applications in sensing, due to their extremely high sensitivity to perturbations. However, this sensitivity is not desirable in other applications such as switching, filtering, and lasing. In [393], a new class of Fano resonances was introduced, whose ultrasharp line shapes is guaranteed and protected by topology. This was achieved by inducing two topological subspaces of even and odd modes in a SSH array of cylinders arranged inside a mono-modal acoustic waveguide. The corresponding even edge mode, originating from multiple scattering of sound, takes the role of the bright state. On the other hand, the odd edge mode, stemming from so-called bound states in the continuum, served as the dark state. By slightly breaking the reflection mirror symmetry of the system, these two topological states were then allowed to couple to each other, creating a Fano line shape (Figure 1e). Thanks to the topological nature of the bright and dark states, such resonance was found to be robust to high levels of disorder. Figure 1f plots the evolution of the Fano line shape versus disorder strength, constituting a direct evidence of its robustness. These Fano resonances are immune to fabrication imperfections and weak disorder, and can be envisioned in other physical platforms, such as optics and microwaves [393].

6.4. *Analog signal processing*

Wave-based analog computing systems have recently been attracted considerable amount of attention for carrying out specialized computational tasks such as differentiation, integration and convolution at extremely fast speeds and low power requirements [394–399]. These advantages are due to the fact that these systems perform the computation at the speed of the wave in the analog domain, without having to digitize the signals, giving rise to real-time and high-throughput computation. Yet, like any other analog system, they suffer from their relatively high sensitivity to perturbations. In [400], the relevance of topological insulators for performing robust signal processing tasks was demonstrated, based on mid-gap one-dimensional topological states. The array was made of cylindrical rods arranged inside an acoustic waveguide. The topological state of such an array induces a Lorentzian transmission spectrum, corresponding to a first-order transfer function. Hence, upon exciting its mid-gap state, the topological system performs time-domain differential equation solving (see Figure 5d, top signal path). Such analog signal processing system is expected to be robust to disorder by virtue of its topological nature. This salient feature is demonstrated in the bottom signal path of Figure 5d, in which the cylinders are randomly shifted away from their original positions. It is observed that the topological analog computing system interestingly maintains its original functionality in the presence of disorder.

7. Discussion and conclusion

In this paper, we reviewed recent findings in the field of classical-wave-based topological insulators. While we discussed a few important technology-oriented applications of topological wave insulators in the previous section, there exists a large variety of reports on other relevant applications, including switching [401–407], modulation [408–410], lensing [411], negative refraction [412], sensing [413], beam splitting [414–418], mode locked fiber lasers [419–424], delay lines [425–427], integrated photonic and phononic devices [428, 429], frequency filters [430], frequency converters [431–433], interferometers [434], and amplifiers [435,436]. It is important to realize that the advantageous properties of topological wave systems, especially in acoustics, are often mitigated by the presence of dissipation losses, imposing certain restrictions on the available bandwidth of operation or propagation length of the topological edge modes. Studying the effect of losses on the topological phases of matter is therefore an emerging direction of research, which has recently inspired the new field of non-Hermitian topological insulators [437–453]. By exploiting the interplay between gain, loss and coupling strengths, such types of insulating phases allow one to go beyond the restrictions of Hermitian topological insulators, especially their sensitivity to absorption losses.

Apart from the Chern insulating phases that are protected by time-reversal symmetry, the remaining topological phases discussed in this review are protected by special symmetries that can be easily broken (like rotational symmetry of the underlying crystal). Enhancing the robustness of topological insulators to disorders that break these symmetries is therefore another important direction, which needs to be pursued. In order to develop defect-immunity engineering at optical frequencies, it may be possible to exploit metatronic techniques [454], so as to optimize the system parameters in a way that it not only benefits from topological protection but it also minimizes its sensitivity to the types of disorder that break the topology of the system.

Exploring topological phases of matter in dimensions higher than what is physically accessible is another promising direction of research [455–458]. In particular, while here we restricted our discussion to two-dimensional and three-dimensional topological phases, there have been several recent reports on topological phases in four dimensions and above, based on the notion of synthetic dimensions [459–473]. Despite the fact that such states have not found specific engineering-oriented applications up to date, they have established an elegant experimental platform, stimulating the deep connection between condensed-matter and elementary particle physics. In general, the idea of exploiting temporal modulations in this context appears to be very rich and not yet fully exploited.

Overall, while to date many of the ideas explored in the context of wave topological insulators have been motivated by physics-driven explorations, the field has a bright future not only in emerging theoretically-driven directions (non-linear, non-Hermitian, etc), but also in the plethora of practical applications of topology in wave engineering (disorder immunity, signal processing, sensing, lasing, etc).

References

[1] L. D. Landau, "On the theory of phase transitions", *Ukr. J. Phys.* **11** (1937), p. 19-32.
[2] F. D. M. Haldane, "Model for a quantum Hall effect without Landau levels: condensed-matter realization of the "parity anomaly"", *Phys. Rev. Lett.* **61** (1988), no. 18, p. 2015.
[3] X.-G. Wen, "Topological orders in rigid states", *Intl J. Modern Phys. B* **4** (1990), no. 02, p. 239-271.
[4] M. Z. Hasan, C. L. Kane, "Colloquium: topological insulators", *Rev. Mod. Phys.* **82** (2010), no. 4, p. 3045.
[5] X.-L. Qi, S.-C. Zhang, "Topological insulators and superconductors", *Rev. Mod. Phys.* **83** (2011), no. 4, p. 1057.
[6] B. A. Bernevig, T. L. Hughes, *Topological Insulators and Topological Superconductors*, Princeton University Press, 2013.
[7] Y. Hatsugai, "Chern number and edge states in the integer quantum Hall effect", *Phys. Rev. Lett.* **71** (1993), no. 22, p. 3697.
[8] C. Wang, A. C. Potter, T. Senthil, "Classification of interacting electronic topological insulators in three dimensions", *Science* **343** (2014), no. 6171, p. 629-631.
[9] C. Nayak *et al.*, "Non-Abelian anyons and topological quantum computation", *Rev. Mod. Phys.* **80** (2008), no. 3, p. 1083.
[10] J. D. Sau *et al.*, "Generic new platform for topological quantum computation using semiconductor heterostructures", *Phys. Rev. Lett.* **104** (2010), no. 4, article ID 040502.
[11] M. Freedman *et al.*, "Topological quantum computation", *Bull. Am. Math. Soc.* **40** (2003), no. 1, p. 31-38.
[12] D. Pesin, A. H. MacDonald, "Spintronics and pseudospintronics in graphene and topological insulators", *Nat. Mater.* **11** (2012), no. 5, p. 409.
[13] L. Šmejkal *et al.*, "Topological antiferromagnetic spintronics", *Nat. Phys.* (2018), p. 1.
[14] M. V. Berry, "Quantal phase factors accompanying adiabatic changes", *Proc. R. Soc. Lond. A. Math. Phys. Sci.* **392** (1984), no. 1802, p. 45-57.
[15] F. D. M. Haldane, S. Raghu, "Possible realization of directional optical waveguides in photonic crystals with broken time-reversal symmetry", *Phys. Rev. Lett.* **100** (2008), no. 1, article ID 013904.
[16] L. Lu, J. D. Joannopoulos, M. Soljačić, "Topological photonics", *Nat. Photonics* **8** (2014), no. 11, p. 821.
[17] A. B. Khanikaev, G. Shvets, "Two-dimensional topological photonics", *Nat. Photonics* **11** (2017), no. 12, p. 763.
[18] T. Ozawa *et al.*, "Topological photonics", *Rev. Mod. Phys.* **91** (2019), no. 1, article ID 015006.
[19] C. Liu *et al.*, "Disorder-induced topological state transition in photonic metamaterials", *Phys. Rev. Lett.* **119** (2017), no. 18, article ID 183901.
[20] S. Barik *et al.*, "A topological quantum optics interface", *Science* **359** (2018), no. 6376, p. 666-668.
[21] W. Gao *et al.*, "Topological photonic phase in chiral hyperbolic metamaterials", *Phys. Rev. Lett.* **114** (2015), no. 3, article ID 037402.
[22] S. Kruk *et al.*, "Edge states and topological phase transitions in chains of dielectric nanoparticles", *Small* **13** (2017), no. 11, article ID 1603190.
[23] C. Yin *et al.*, "Realizing topological edge states in a silicon nitride microring-based photonic integrated circuit", *Opt. Lett.* **41** (2016), no. 20, p. 4791-4794.
[24] J. Noh *et al.*, "Topological protection of photonic mid-gap defect modes", *Nat. Photonics* **12** (2018), no. 7, p. 408.
[25] S. R. Pocock *et al.*, "Topological plasmonic chain with retardation and radiative effects", *Acs Photonics* **5** (2018), no. 6, p. 2271-2279.
[26] A. V. Poshakinskiy, A. N. Poddubny, "Optomechanical Kerker effect", *Phys. Rev. X* **9** (2019), no. 1, article ID 011008.
[27] J. Perczel *et al.*, "Topological quantum optics in two-dimensional atomic arrays", *Phys. Rev. Lett.* **119** (2017), no. 2, article ID 023603.
[28] B. Yang *et al.*, "Direct observation of topological surface-state arcs in photonic metamaterials", *Nat. Commun.* **8** (2017), no. 1, p. 97.
[29] W. Tan *et al.*, "Photonic simulation of topological excitations in metamaterials", *Sci. Rep.* **4** (2014), p. 3842.
[30] X.-D. Chen, X.-T. He, J.-W. Dong, "All-dielectric layered photonic topological insulators", *Laser Photonics Rev.* **13** (2019), no. 8, article ID 1900091.
[31] J. Yuen-Zhou *et al.*, "Topologically protected excitons in porphyrin thin films", *Nat. Mater.* **13** (2014), no. 11, p. 1026.
[32] T. Ma, G. Shvets, "Scattering-free edge states between heterogeneous photonic topological insulators", *Phys. Rev. B* **95** (2017), no. 16, article ID 165102.
[33] D. A. Jacobs *et al.*, "Photonic topological Chern insulators based on Tellegen metacrystals", *New J. Phys.* **17** (2015), no. 12, article ID 125015.
[34] R. E. Christiansen, F. Wang, O. Sigmund, "Topological insulators by topology optimization", *Phys. Rev. Lett.* **122** (2019), no. 23, article ID 234502.
[35] F.-F. Li *et al.*, "Topological light-trapping on a dislocation", *Nat. Commun.* **9** (2018), no. 1, p. 2462.
[36] T. Karzig *et al.*, "Topological polaritons", *Phys. Rev. X* **5** (2015), no. 3, article ID 031001.

[37] M. C. Rechtsman *et al.*, "Topological creation and destruction of edge states in photonic graphene", *Phys. Rev. Lett.* **111** (2013), no. 10, article ID 103901.
[38] Q. Huang *et al.*, "Observation of a topological edge state in the X-ray band", *Laser Photonics Rev.* **13** (2019), no. 6, article ID 1800339.
[39] F. Liu, H.-Y. Deng, K. Wakabayashi, "Topological photonic crystals with zero Berry curvature", *Phys. Rev. B* **97** (2018), no. 3, article ID 035442.
[40] J. Han, C. Gneiting, D. Leykam, "Helical transport in coupled resonator waveguides", *Phys. Rev. B* **99** (2019), no. 22, article ID 224201.
[41] F. Lindel *et al.*, "Inducing and controlling rotation on small objects using photonic topological materials", *Phys. Rev. B* **98** (2018), no. 14, article ID 144101.
[42] L. Xu *et al.*, "Accidental degeneracy in photonic bands and topological phase transitions in two-dimensional core-shell dielectric photonic crystals", *Opt. Express* **24** (2016), no. 16, p. 18059-18071.
[43] B.-Y. Xie *et al.*, "Photonics meets topology", *Opt. Express* **26** (2018), no. 19, p. 24531-24550.
[44] M. Bello *et al.*, "Unconventional quantum optics in topological waveguide QED", *Sci. Adv.* **5** (2019), no. 7, article ID eaaw0297.
[45] Y. Wang *et al.*, "Topological protection of two-photon quantum correlation on a photonic chip", *Optica* **6** (2019), no. 8, p. 955-960.
[46] T. Dubček *et al.*, "The Harper–Hofstadter Hamiltonian and conical diffraction in photonic lattices with grating assisted tunneling", *New J. Phys.* **17** (2015), no. 12, article ID 125002.
[47] Z. A. Kudyshev *et al.*, "Photonic topological phase transition on demand", *Nanophotonics* **8** (2019), p. 1349-1356.
[48] S. A. Sato *et al.*, "Microscopic theory for the light-induced anomalous Hall effect in graphene", *Phys. Rev. B* **99** (2019), no. 21, article ID 214302.
[49] Y. Li, J. Mei, "Double Dirac cones in two-dimensional dielectric photonic crystals", *Opt. Express* **23** (2015), no. 9, p. 12089-12099.
[50] X.-C. Sun *et al.*, "Two-dimensional topological photonic systems", *Prog. Quantum Electron.* **55** (2017), p. 52-73.
[51] L. Wang *et al.*, "Subwavelength topological edge states based on localized spoof surface plasmonic metaparticle arrays", *Opt. Express* **27** (2019), no. 10, p. 14407-14422.
[52] J. W. McIver *et al.*, "Control over topological insulator photocurrents with light polarization", *Nat. Nanotechnol.* **7** (2012), no. 2, p. 96.
[53] Y. Long *et al.*, "Inverse design of photonic topological state via machine learning", *Appl. Phys. Lett.* **114** (2019), no. 18, article ID 181105.
[54] P. Di Pietro *et al.*, "Observation of Dirac plasmons in a topological insulator", *Nat. Nanotechnol.* **8** (2013), no. 8, p. 556.
[55] F. Gao *et al.*, "Probing topological protection using a designer surface plasmon structure", *Nat. Commun.* **7** (2016), article ID 11619.
[56] Y. Ke *et al.*, "Topological phase transitions and thouless pumping of light in photonic waveguide arrays", *Laser Photonics Rev.* **10** (2016), no. 6, p. 995-1001.
[57] M. S. Rider *et al.*, "A perspective on topological nanophotonics: current status and future challenges", *J. Appl. Phys.* **125** (2019), no. 12, article ID 120901.
[58] M. I. Shalaev, W. Walasik, N. M. Litchinitser, "Optically tunable topological photonic crystal", *Optica* **6** (2019), no. 7, p. 839-844.
[59] S. Klembt *et al.*, "Exciton-polariton topological insulator", *Nature* **562** (2018), no. 7728, p. 552.
[60] X. Yao, M. Tokman, A. Belyanin, "Efficient nonlinear generation of THz plasmons in graphene and topological insulators", *Phys. Rev. Lett.* **112** (2014), no. 5, article ID 055501.
[61] F. Cardano *et al.*, "Detection of Zak phases and topological invariants in a chiral quantum walk of twisted photons", *Nat. Commun.* **8** (2017), article ID 15516.
[62] T. Kitagawa *et al.*, "Observation of topologically protected bound states in photonic quantum walks", *Nat. Commun.* **3** (2012), p. 882.
[63] N. P. Mitchell *et al.*, "Amorphous topological insulators constructed from random point sets", *Nat. Phys.* **14** (2018), no. 4, p. 380.
[64] E. Lustig *et al.*, "Curved-space topological phases in photonic lattices", *Phys. Rev. A* **96** (2017), no. 4, article ID 041804.
[65] P. N. Dyachenko *et al.*, "Controlling thermal emission with refractory epsilon-near-zero metamaterials via topological transitions", *Nat. Commun.* **7** (2016), article ID 11809.
[66] T. Ma, G. Shvets, "All-Si valley-Hall photonic topological insulator", *New J. Phys.* **18** (2016), no. 2, article ID 025012.
[67] B. Yang *et al.*, "Topological states in amorphous magnetic photonic lattices", *Phys. Rev. B* **99** (2019), no. 4, article ID 045307.
[68] A. Girschik, F. Libisch, S. Rotter, "Percolating states in the topological Anderson insulator", *Phys. Rev. B* **91** (2015), no. 21, article ID 214204.

[69] J.-P. Xia *et al.*, "Programmable coding acoustic topological insulator", *Adv. Mater.* **30** (2018), no. 46, article ID 1805002.

[70] C. Brendel *et al.*, "Snowflake phononic topological insulator at the nanoscale", *Phys. Rev. B* **97** (2018), no. 2, article ID 020102.

[71] Z. Yang *et al.*, "Strain-induced gauge field and Landau levels in acoustic structures", *Phys. Rev. Lett.* **118** (2017), no. 19, article ID 194301.

[72] Y. Meng *et al.*, "Designing topological interface states in phononic crystals based on the full phase diagrams", *New J. Phys.* **20** (2018), no. 7, article ID 073032.

[73] J. Chen *et al.*, "Self-ordering induces multiple topological transitions for in-plane bulk waves in solid phononic crystals", *Phys. Rev. B* **98** (2018), no. 1, article ID 014302.

[74] F. Zangeneh-Nejad, R. Fleury, "Active times for acoustic metamaterials", *Rev. Phys.* (2019), article ID 100031.

[75] X. Ni *et al.*, "Topologically protected one-way edge mode in networks of acoustic resonators with circulating air flow", *New J. Phys.* **17** (2015), no. 5, article ID 053016.

[76] X. Wen *et al.*, "Acoustic Landau quantization and quantum-Hall-like edge states", *Nat. Phys.* **15** (2019), p. 352-356.

[77] D. Zhao *et al.*, "Topological interface modes in local resonant acoustic systems", *Phys. Rev. B* **98** (2018), no. 1, article ID 014110.

[78] M.-J. Tuo *et al.*, "Twist-projected two-dimensional acoustic topological insulators", *Phys. Rev. B* **99** (2019), no. 20, article ID 205432.

[79] L.-Y. Zheng *et al.*, "Observation of edge waves in a two-dimensional Su–Schrieffer–Heeger acoustic network", *Phys. Rev. Appl.* **12** (2019), no. 3, article ID 034014.

[80] G. Arregui *et al.*, "Coherent generation and detection of acoustic phonons in topological nanocavities", *APL Photonics* **4** (2019), no. 3, article ID 030805.

[81] G. Baardink *et al.*, "Localizing softness and stress along loops in 3D topological metamaterials", *Proc. Natl Acad. Sci. USA* **115** (2018), no. 3, p. 489-494.

[82] J. Ma *et al.*, "Optically Controlled Topologically Protected Acoustic Wave Amplification", *IEEE J. Selected Topics Quantum Electron.* **26** (2019), p. 1-10.

[83] X. Zhang *et al.*, "Topological sound", *Commun. Phys.* **1** (2018), no. 1, p. 97.

[84] J. Yin *et al.*, "Band transition and topological interface modes in 1D elastic phononic crystals", *Sci. Rep.* **8** (2018), no. 1, p. 6806.

[85] V. Peano *et al.*, "Topological phases of sound and light", *Phys. Rev. X* **5** (2015), no. 3, article ID 031011.

[86] S. Shankar, M. J. Bowick, M. C. Marchetti, "Topological sound and flocking on curved surfaces", *Phys. Rev. X* **7** (2017), no. 3, article ID 031039.

[87] B. Xie *et al.*, "Acoustic topological transport and refraction in a Kekulé lattice", *Phys. Rev. Appl.* **11** (2019), no. 4, article ID 044086.

[88] Y. Liu *et al.*, "Pseudospins and topological effects of phonons in a Kekulé lattice", *Phys. Rev. Lett.* **119** (2017), no. 25, article ID 255901.

[89] H. Abbaszadeh *et al.*, "Sonic Landau levels and synthetic gauge fields in mechanical metamaterials", *Phys. Rev. Lett.* **119** (2017), no. 19, article ID 195502.

[90] Z.-G. Chen, Y. Wu, "Tunable topological phononic crystals", *Phys. Rev. Appl.* **5** (2016), no. 5, article ID 054021.

[91] A. Darabi, M. J. Leamy, "Reconfigurable topological insulator for elastic waves", *J. Acoust. Soc. Am.* **146** (2019), no. 1, p. 773-781.

[92] Z.-Y. Ong, C. H. Lee, "Transport and localization in a topological phononic lattice with correlated disorder", *Phys. Rev. B* **94** (2016), no. 13, article ID 134203.

[93] G. Gupta *et al.*, "Role of acoustic phonons in Bi_2Se_3 topological insulator slabs: a quantum transport investigation", *Phys. Rev. B* **89** (2014), no. 24, article ID 245419.

[94] Z. Yang, F. Gao, B. Zhang, "Topological water wave states in a one-dimensional structure", *Sci. Rep.* **6** (2016), article ID 29202.

[95] S.-Y. Huo, J.-J. Chen, H.-B. Huang, "Topologically protected edge states for out-of-plane and in-plane bulk elastic waves", *J. Phys.: Condens. Matter* **30** (2018), no. 14, article ID 145403.

[96] G. Ma, M. Xiao, C. T. Chan, "Topological phases in acoustic and mechanical systems", *Nat. Rev. Phys.* **1** (2019), p. 281-294.

[97] K. Saha, I. Garate, "Phonon-induced topological insulation", *Phys. Rev. B* **89** (2014), no. 20, article ID 205103.

[98] T. Lee, H. Iizuka, "Bragg scattering based acoustic topological transition controlled by local resonance", *Phys. Rev. B* **99** (2019), no. 6, article ID 064305.

[99] Y. Liu *et al.*, "Model for topological phononics and phonon diode", *Phys. Rev. B* **96** (2017), no. 6, article ID 064106.

[100] Z. Yu, Z. Ren, J. Lee, "Phononic topological insulators based on six-petal holey silicon structures", *Sci. Rep.* **9** (2019), no. 1, p. 1805.

[101] R. Süsstrunk, S. D. Huber, "Observation of phononic helical edge states in a mechanical topological insulator", *Science* **349** (2015), no. 6243, p. 47-50.

[102] S. D. Huber, "Topological mechanics", *Nat. Phys.* **12** (2016), no. 7, p. 621.
[103] H. Chen, H. Nassar, G. Huang, "Topological mechanics of edge waves in Kagome lattices", *preprint*, arXiv:1802.04404 (2018).
[104] B. Liu *et al.*, "Topological kinematics of origami metamaterials", *Nat. Phys.* **14** (2018), no. 8, p. 811.
[105] A. S. Meeussen, J. Paulose, V. Vitelli, "Geared topological metamaterials with tunable mechanical stability", *Phys. Rev. X* **6** (2016), no. 4, article ID 041029.
[106] T. Tian *et al.*, "Observation of dynamical phase transitions in a topological nanomechanical system", *Phys. Rev. B* **100** (2019), no. 2, article ID 024310.
[107] J. Cha, K. W. Kim, C. Daraio, "Experimental realization of on-chip topological nanoelectromechanical metamaterials", *Nature* **564** (2018), no. 7735, p. 229.
[108] Y.-W. Tsai *et al.*, "Topological phase transition in a one-dimensional elastic string system", *Crystals* **9** (2019), no. 6, p. 313.
[109] Y. Zhou *et al.*, "Kink-antikink asymmetry and impurity interactions in topological mechanical chains", *Phys. Rev. E* **95** (2017), no. 2, article ID 022202.
[110] E. Prodan *et al.*, "Dynamical Majorana edge modes in a broad class of topological mechanical systems", *Nat. Commun.* **8** (2017), article ID 14587.
[111] J. Paulose, B. G.-g. Chen, V. Vitelli, "Topological modes bound to dislocations in mechanical metamaterials", *Nat. Phys.* **11** (2015), no. 2, p. 153.
[112] J. Köpfler *et al.*, "Topologically protected twist edge states for a resonant mechanical laser-beam scanner", *Phys. Rev. Appl.* **11** (2019), no. 3, article ID 034059.
[113] P. Deymier, K. Runge, "One-dimensional mass-spring chains supporting elastic waves with non-conventional topology", *Crystals* **6** (2016), no. 4, p. 44.
[114] R. Chaunsali, F. Li, J. Yang, "Stress wave isolation by purely mechanical topological phononic crystals", *Sci. Rep.* **6** (2016), article ID 30662.
[115] M. Brandenbourger *et al.*, "Non-reciprocal robotic metamaterials", *Nat. Commun.* **10** (2019), no. 1, p. 1-8.
[116] S. M. Young *et al.*, "Theoretical investigation of the evolution of the topological phase of Bi_2Se_3 under mechanical strain", *Phys. Rev. B* **84** (2011), no. 8, article ID 085106.
[117] Y.-T. Wang, P.-G. Luan, S. Zhang, "Coriolis force induced topological order for classical mechanical vibrations", *New J. Phys.* **17** (2015), no. 7, article ID 073031.
[118] D. Z. Rocklin *et al.*, "Transformable topological mechanical metamaterials", *Nat. Commun.* **8** (2017), article ID 14201.
[119] G. Wang, H. Xu, Y.-C. Lai, "Mechanical topological semimetals with massless quasiparticles and a finite Berry curvature", *Phys. Rev. B* **95** (2017), no. 23, article ID 235159.
[120] J. Attig *et al.*, "Topological mechanics from supersymmetry", *Phys. Rev. Res.* **1** (2019), no. 3, article ID 032047.
[121] Z. Xiong *et al.*, "Topological node lines in mechanical metacrystals", *Phys. Rev. B* **97** (2018), no. 18, article ID 180101.
[122] H. Chen, H. Nassar, G. L. Huang, "A study of topological effects in 1D and 2D mechanical lattices", *J. Mech. Phys. Solids* **117** (2018), p. 22-36.
[123] M. Fruchart, D. Carpentier, "An introduction to topological insulators", *C. R. Phys.* **14** (2013), no. 9–10, p. 779-815.
[124] J. K. Asbóth, L. Oroszlány, A. Pályi, "A short course on topological insulators", *Lecture Notes in Physics* **919** (2016), p. 166.
[125] P. A. Kalozoumis *et al.*, "Finite-size effects on topological interface states in one-dimensional scattering systems", *Phys. Rev. A* **98** (2018), no. 2, article ID 023838.
[126] C. E. Whittaker *et al.*, "Effect of photonic spin-orbit coupling on the topological edge modes of a Su–Schrieffer–Heeger chain", *Phys. Rev. B* **99** (2019), no. 8, article ID 081402.
[127] L. Ge *et al.*, "Topological phase transition and interface states in hybrid plasmonic-photonic systems", *J. Opt.* **19** (2017), no. 6, p. 06LT02.
[128] C. L. Kane, T. C. Lubensky, "Topological boundary modes in isostatic lattices", *Nat. Phys.* **10** (2014), no. 1, p. 39.
[129] Y. Hadad, V. Vitelli, A. Alu, "Solitons and propagating domain walls in topological resonator arrays", *ACS Photonics* **4** (2017), no. 8, p. 1974-1979.
[130] B. Midya, L. Feng, "Topological multiband photonic superlattices", *Phys. Rev. A* **98** (2018), no. 4, article ID 043838.
[131] Q. Cheng *et al.*, "Topologically protected interface mode in plasmonic waveguide arrays", *Laser Photonics Rev.* **9** (2015), no. 4, p. 392-398.
[132] C. W. Ling *et al.*, "Topological edge plasmon modes between diatomic chains of plasmonic nanoparticles", *Opt. Express* **23** (2015), no. 3, p. 2021-2031.
[133] F. Bleckmann *et al.*, "Spectral imaging of topological edge states in plasmonic waveguide arrays", *Phys. Rev. B* **96** (2017), no. 4, article ID 045417.
[134] Z. Zhang *et al.*, "Experimental realization of multiple topological edge states in a 1D photonic lattice", *Laser Photonics Rev.* **13** (2019), no. 2, article ID 1800202.

[135] R. K. Pal, J. Vila, M. Ruzzene, "Topologically protected edge states in mechanical metamaterials", *Adv. Crystals Elastic Metamaterials* **52** (2019), p. 147.

[136] A. Altland, M. R. Zirnbauer, "Nonstandard symmetry classes in mesoscopic normal-superconducting hybrid structures", *Phys. Rev. B* **55** (1997), no. 2, p. 1142.

[137] P. St-Jean *et al.*, "Lasing in topological edge states of a one-dimensional lattice", *Nat. Photonics* **11** (2017), no. 10, p. 651.

[138] M. Xiao *et al.*, "Geometric phase and band inversion in periodic acoustic systems", *Nat. Phys.* **11** (2015), no. 3, p. 240.

[139] M. Parto *et al.*, "Edge-mode lasing in 1D topological active arrays", *Phys. Rev. Lett.* **120** (2018), no. 11, article ID 113901.

[140] D. Woolard, J. L. Jensen, *Spectral Sensing Research for Water Monitoring Applications and Frontier Science and Technology for Chemical, Biological and Radiological Defense, Volume 48*, World Scientific, 2008.

[141] Y. Zhang *et al.*, "Experimental observation of the quantum Hall effect and Berry's phase in graphene", *Nature* **438** (2005), no. 7065, p. 201.

[142] Z. Wang *et al.*, "Observation of unidirectional backscattering-immune topological electromagnetic states", *Nature* **461** (2009), no. 7265, p. 772.

[143] W. Śmigaj *et al.*, "Magneto-optical circulator designed for operation in a uniform external magnetic field", *Opt. Lett.* **35** (2010), no. 4, p. 568-570.

[144] R. Fleury *et al.*, "Sound isolation and giant linear nonreciprocity in a compact acoustic circulator", *Science* **343** (2014), no. 6170, p. 516-519.

[145] A. B. Khanikaev *et al.*, "Topologically robust sound propagation in an angular-momentum-biased graphene-like resonator lattice", *Nat. Commun.* **6** (2015), p. 8260.

[146] Z. Yang *et al.*, "Topological acoustics", *Phys. Rev. Lett.* **114** (2015), no. 11, article ID 114301.

[147] A. Souslov *et al.*, "Topological waves in fluids with odd viscosity", *Phys. Rev. Lett.* **122** (2019), no. 12, article ID 128001.

[148] A. Souslov *et al.*, "Topological sound in active-liquid metamaterials", *Nat. Phys.* **13** (2017), no. 11, p. 1091.

[149] Y. Ding *et al.*, "Experimental demonstration of acoustic Chern insulators", *Phys. Rev. Lett.* **122** (2019), no. 1, article ID 014302.

[150] L. M. Nash *et al.*, "Topological mechanics of gyroscopic metamaterials", *Proc. Natl Acad. Sci. USA* **112** (2015), no. 47, p. 14495-14500.

[151] C. L. Kane, E. J. Mele, "Quantum spin Hall effect in graphene", *Phys. Rev. Lett.* **95** (2005), no. 22, article ID 226801.

[152] B. A. Bernevig, T. L. Hughes, S.-C. Zhang, "Quantum spin Hall effect and topological phase transition in HgTe quantum wells", *Science* **314** (2006), no. 5806, p. 1757-1761.

[153] R. K. Pal, M. Schaeffer, M. Ruzzene, "Helical edge states and topological phase transitions in phononic systems using bi-layered lattices", *J. Appl. Phys.* **119** (2016), no. 8, article ID 084305.

[154] X.-Y. Zhu *et al.*, "Z_2 topological edge state in honeycomb lattice of coupled resonant optical waveguides with a flat band", *Opt. Express* **26** (2018), no. 19, p. 24307-24317.

[155] M. L. N. Chen *et al.*, "Pseudospin-polarized topological line defects in dielectric photonic crystals", *IEEE Trans. Antennas Propagation* **68** (2019), p. 609-613.

[156] H. Zhong *et al.*, "Topological insulator properties of photonic kagome helical waveguide arrays", *Results Phys.* **12** (2019), p. 996-1001.

[157] H. Xiong *et al.*, "Polarization-resolved edge states in terahertz topological photonic crystal", *Opt. Express* **27** (2019), no. 16, p. 22819-22826.

[158] O. Gröning *et al.*, "Engineering of robust topological quantum phases in graphene nanoribbons", *Nature* **560** (2018), no. 7717, p. 209.

[159] A. P. Slobozhanyuk *et al.*, "Enhanced photonic spin Hall effect with subwavelength topological edge states", *Laser Photonics Rev.* **10** (2016), no. 4, p. 656-664.

[160] X.-C. Sun *et al.*, "Photonic topological states in a two-dimensional gyrotropic photonic crystal", *Crystals* **9** (2019), no. 3, p. 137.

[161] V. K. Kozin *et al.*, "Topological metamaterials based on polariton rings", *Phys. Rev. B* **98** (2018), no. 12, article ID 125115.

[162] R. E. Christiansen *et al.*, "Designing photonic topological insulators with quantum-spin-Hall edge states using topology optimization", *Nanophotonics* **8** (2019), p. 1363-1369.

[163] K. Y. Bliokh, D. Smirnova, F. Nori, "Quantum spin Hall effect of light", *Science* **348** (2015), no. 6242, p. 1448-1451.

[164] C. He *et al.*, "Acoustic topological insulator and robust one-way sound transport", *Nat. Phys.* **12** (2016), no. 12, p. 1124.

[165] S. S. Nanthakumar *et al.*, "Inverse design of quantum spin hall-based phononic topological insulators", *J. Mech. Phys. Solids* **125** (2019), p. 550-571.

[166] D. Jia *et al.*, "Pseudospin-dependent acoustic topological insulator by airborne sonic crystals with a triangular lattice", *Appl. Phys. Express* **12** (2019), no. 4, article ID 044003.

[167] H. Chen *et al.*, "Elastic quantum spin Hall effect in kagome lattices", *Phys. Rev. B* **98** (2018), no. 9, article ID 094302.

[168] F. Ju, Y. Cheng, X. Liu, "Acoustic spin Hall-like effect in hyperbolic metamaterials controlled by the helical wave", *Sci. Rep.* **8** (2018), no. 1, article ID 11113.

[169] B.-Z. Xia *et al.*, "Topological phononic insulator with robust pseudospin-dependent transport", *Phys. Rev. B* **96** (2017), no. 9, article ID 094106.

[170] Y. Liu, Y. Xu, W. Duan, "Phononic topological insulators with tunable pseudospin physics", *preprint*, arXiv:1809.05721 (2018).

[171] X.-F. Zhu *et al.*, "Topologically protected acoustic helical edge states and interface states in strongly coupled metamaterial ring lattices", *preprint*, arXiv:1508.06243 (2015).

[172] S. Wang, G. Ma, C. T. Chan, "Topological transport of sound mediated by spin-redirection geometric phase", *Sci. Adv.* **4** (2018), no. 2, article ID eaaq1475.

[173] A. Slobozhanyuk *et al.*, "Three-dimensional all-dielectric photonic topological insulator", *Nat. Photonics* **11** (2017), no. 2, p. 130.

[174] C. He *et al.*, "Photonic topological insulator with broken time-reversal symmetry", *Proc. Natl Acad. Sci. USA* **113** (2016), no. 18, p. 4924-4928.

[175] L.-y. Feng *et al.*, "Reconfigurable topological phononic crystal slabs", *Phys. Lett. A* **382** (2018), no. 39, p. 2880-2885.

[176] Z. Gao *et al.*, "Flexible photonic topological insulator", *Adv. Opt. Mater.* **6** (2018), no. 17, article ID 1800532.

[177] S. H. Mousavi, A. B. Khanikaev, Z. Wang, "Topologically protected elastic waves in phononic metamaterials", *Nat. Commun.* **6** (2015), p. 8682.

[178] Y. Yang, Z. H. Hang, "Topological whispering gallery modes in two-dimensional photonic crystal cavities", *Opt. Express* **26** (2018), no. 16, p. 21235-21241.

[179] Y. Li *et al.*, "Topological LC-circuits based on microstrips and observation of electromagnetic modes with orbital angular momentum", *Nat. Commun.* **9** (2018), no. 1, p. 4598.

[180] J. Mei, Z. Chen, Y. Wu, "Pseudo-time-reversal symmetry and topological edge states in two-dimensional acoustic crystals", *Sci. Rep.* **6** (2016), article ID 32752.

[181] Y. Deng *et al.*, "Observation of zone folding induced acoustic topological insulators and the role of spin-mixing defects", *Phys. Rev. B* **96** (2017), no. 18, article ID 184305.

[182] C. He *et al.*, "Topological phononic states of underwater sound based on coupled ring resonators", *Appl. Phys. Lett.* **108** (2016), no. 3, article ID 031904.

[183] H. Dai *et al.*, "Subwavelength acoustic topological edge states realized by zone folding and the role of boundaries selection", *J. Appl. Phys.* **124** (2018), no. 17, article ID 175107.

[184] S. Li *et al.*, "Observation of elastic topological states in soft materials", *Nat. Commun.* **9** (2018), no. 1, p. 1370.

[185] X.-D. Chen *et al.*, "Accidental double dirac cones and robust edge states in topological anisotropic photonic crystals", *Laser Photonics Rev.* **12** (2018), no. 11, article ID 1800073.

[186] Y. Zhou, P. R. Bandaru, D. F. Sievenpiper, "Quantum-spin-Hall topological insulator in a spring-mass system", *New J. Phys.* **20** (2018), no. 12, article ID 123011.

[187] A. B. Khanikaev *et al.*, "Photonic topological insulators", *Nat. Mater.* **12** (2013), no. 3, p. 233.

[188] M. Miniaci *et al.*, "Experimental observation of topologically protected helical edge modes in patterned elastic plates", *Phys. Rev. X* **8** (2018), no. 3, article ID 031074.

[189] E. Martini, M. G. Silveirinha, S. Maci, "Exact solution for the protected TEM edge mode in a PTD-symmetric parallel-plate waveguide", *IEEE Trans. Antennas Propagation* **67** (2018), no. 2, p. 1035-1044.

[190] M. G. Silveirinha, "P. T. D symmetry-protected scattering anomaly in optics", *Phys. Rev. B* **95** (2017), no. 3, article ID 035153.

[191] L.-H. Wu, X. Hu, "Scheme for achieving a topological photonic crystal by using dielectric material", *Phys. Rev. Lett.* **114** (2015), no. 22, article ID 223901.

[192] S. Yves *et al.*, "Crystalline metamaterials for topological properties at subwavelength scales", *Nat. Commun.* **8** (2017), article ID 16023.

[193] L. Wang *et al.*, "The existence of topological edge states in honeycomb plasmonic lattices", *New J. Phys.* **18** (2016), no. 10, article ID 103029.

[194] S. Barik *et al.*, "Two-dimensionally confined topological edge states in photonic crystals", *New J. Phys.* **18** (2016), no. 11, article ID 113013.

[195] Y. Yang *et al.*, "Visualization of a unidirectional electromagnetic waveguide using topological photonic crystals made of dielectric materials", *Phys. Rev. Lett.* **120** (2018), no. 21, article ID 217401.

[196] M. I. Shalaev *et al.*, "Robust topologically protected transport in photonic crystals at telecommunication wavelengths", *Nat. Nanotechnol.* **14** (2019), no. 1, p. 31.

[197] M. Honari-Latifpour, Y. Leila, "Topological plasmonic edge states in a planar array of metallic nanoparticles", *Nanophotonics* **8** (2019), p. 799-806.

[198] S. Wu, Y. Wu, J. Mei, "Topological helical edge states in water waves over a topographical bottom", *New J. Phys.* **20** (2018), no. 2, article ID 023051.

[199] R. Chaunsali, C.-W. Chen, J. Yang, "Experimental demonstration of topological waveguiding in elastic plates with local resonators", *New J. Phys.* **20** (2018), no. 11, article ID 113036.
[200] Y. Chen, X. Liu, G. Hu, "Topological phase transition in mechanical honeycomb lattice", *J. Mech. Phys. Solids* **122** (2019), p. 54-68.
[201] S.-Y. Yu *et al.*, "Elastic pseudospin transport for integratable topological phononic circuits", *Nat. Commun.* **9** (2018), no. 1, p. 3072.
[202] Z. Zhang *et al.*, "Topological creation of acoustic pseudospin multipoles in a flow-free symmetry-broken metamaterial lattice", *Phys. Rev. Lett.* **118** (2017), no. 8, article ID 084303.
[203] Z. Zhang *et al.*, "Experimental verification of acoustic pseudospin multipoles in a symmetry-broken snowflakelike topological insulator", *Phys. Rev. B* **96** (2017), no. 24, article ID 241306.
[204] Z.-G. Geng *et al.*, "Topologically protected edge transport of sound in coupled cavities of a modified honeycomb lattice", *J. Phys.: Condens. Matter* **30** (2018), no. 34, article ID 345401.
[205] S. Yves *et al.*, "Topological acoustic polaritons: robust sound manipulation at the subwavelength scale", *New J. Phys.* **19** (2017), no. 7, article ID 075003.
[206] B. Bradlyn *et al.*, "Topological quantum chemistry", *Nature* **547** (2017), no. 7663, p. 298.
[207] B. Orazbayev, R. Fleury, "Quantitative robustness analysis of topological edge modes in C6 and Valley-Hall metamaterial waveguides", *Nanophotonics* **8** (2019), p. 1433-1441.
[208] X.-T. He *et al.*, "A silicon-on-insulator slab for topological valley transport", *Nat. Commun.* **10** (2019), no. 1, p. 872.
[209] Z. Zhu *et al.*, "Negative refraction and partition in acoustic valley materials of a square lattice", *Phys. Rev. Appl.* **12** (2019), no. 2, article ID 024007.
[210] L. Ye *et al.*, "Observation of valley-selective microwave transport in photonic crystals", *Appl. Phys. Lett.* **111** (2017), no. 25, article ID 251107.
[211] X. Han *et al.*, "Experimental demonstration of acoustic valley hall topological insulators with the robust selection of C 3v-symmetric scatterers", *Phys. Rev. Appl.* **12** (2019), no. 1, article ID 014046.
[212] X. Wu *et al.*, "Direct observation of valley-polarized topological edge states in designer surface plasmon crystals", *Nat. Commun.* **8** (2017), no. 1, p. 1304.
[213] Y. Deng, Y. Jing, "A comparison study between topological insulators based on valley Hall and quantum spin Hall effects", *J. Acoust. Soc. Am.* **145** (2019), no. 3, p. 1762-1762.
[214] D. Song *et al.*, "Valley vortex states and degeneracy lifting via photonic higher-band excitation", *Phys. Rev. Lett.* **122** (2019), no. 12, article ID 123903.
[215] Z. Gao *et al.*, "Valley surface-wave photonic crystal and its bulk/edge transport", *Phys. Rev. B* **96** (2017), no. 20, article ID 201402.
[216] Q. Chen *et al.*, "Valley-Hall photonic topological insulators with dual-band kink states", *Adv. Optical Mater.* (2019), article ID 1900036.
[217] R. K. Pal, M. Ruzzene, "Edge waves in plates with resonators: an elastic analogue of the quantum valley Hall effect", *New J. Phys.* **19** (2017), no. 2, article ID 025001.
[218] C. He *et al.*, "Three-dimensional topological acoustic crystals with pseudospin-valley coupled saddle surface states", *Nat. Commun.* **9** (2018), no. 1, p. 4555.
[219] T.-W. Liu, F. Semperlotti, "Experimental evidence of robust acoustic valley Hall edge states in a nonresonant topological elastic waveguide", *Phys. Rev. Appl.* **11** (2019), no. 1, article ID 014040.
[220] T.-W. Liu, F. Semperlotti, "Tunable acoustic valley-Hall edge states in reconfigurable phononic elastic waveguides", *Phys. Rev. Appl.* **9** (2018), no. 1, article ID 014001.
[221] X. Wu *et al.*, "Interlayer topological transport and devices based on layer pseudospins in photonic valley-Hall phases", *Adv. Opt. Mater.* **7** (2019), article ID 1900872.
[222] J. Lu *et al.*, "Valley topological phases in bilayer sonic crystals", *Phys. Rev. Lett.* **120** (2018), no. 11, article ID 116802.
[223] J.-J. Chen *et al.*, "Topological valley transport of plate-mode waves in a homogenous thin plate with periodic stubbed surface", *AIP Adv.* **7** (2017), no. 11, article ID 115215.
[224] Y. Shen *et al.*, "Valley-projected edge modes observed in underwater sonic crystals", *Appl. Phys. Lett.* **114** (2019), no. 2, article ID 023501.
[225] H. Dai, B. Xia, D. Yu, "Temperature-controlled tunable underwater acoustic topological insulators", *J. Appl. Phys.* **125** (2019), no. 23, article ID 235105.
[226] J. Lu *et al.*, "Valley vortex states in sonic crystals", *Phys. Rev. Lett.* **116** (2016), no. 9, article ID 093901.
[227] J. Vila, R. K. Pal, M. Ruzzene, "Observation of topological valley modes in an elastic hexagonal lattice", *Phys. Rev. B* **96** (2017), no. 13, article ID 134307.
[228] H. Zhu, T.-W. Liu, F. Semperlotti, "Design and experimental observation of valley-Hall edge states in diatomic-graphene-like elastic waveguides", *Phys. Rev. B* **97** (2018), no. 17, article ID 174301.
[229] M. Miniaci *et al.*, "Valley-based splitting of topologically protected helical waves in elastic plates", *Phys. Rev. B* **100** (2019), no. 2, article ID 024304.

[230] Z. Yu, Z. Ren, J. Lee, "Phononic topological insulators based on six-petal holey silicon structures", *Sci. Rep.* **9** (2019), no. 1, p. 1805.
[231] Z.-G. Geng *et al.*, "Mirror-symmetry induced topological valley transport along programmable boundaries in a hexagonal sonic crystal", *J. Phys.: Condens. Matter* **31** (2019), no. 24, article ID 245403.
[232] B.-Z. Xia *et al.*, "Observation of valleylike edge states of sound at a momentum away from the high-symmetry points", *Phys. Rev. B* **97** (2018), no. 15, article ID 155124.
[233] C. Chen *et al.*, "Observation of topological locally resonate and Bragg edge modes in a two-dimensional slit-typed sonic crystal", *Appl. Phys. Express* **12** (2019), no. 9, article ID 097001.
[234] M. Chen *et al.*, "Tunable Dirac cones in two-dimensional acoustic metamaterials with matryoshka structure", *J. Acoust. Soc. Am.* **146** (2019), no. 1, p. 767-772.
[235] Y.-F. Tang *et al.*, "Topological phononic crystals with tunable interface state based on local resonance", *Appl. Phys. Express* **12** (2019), no. 9, article ID 094002.
[236] Y. Yang, Z. Yang, B. Zhang, "Acoustic valley edge states in a graphene-like resonator system", *J. Appl. Phys.* **123** (2018), no. 9, article ID 091713.
[237] G. G. Gentili *et al.*, "Towards topological protection based millimeter wave devices", *Phys. Rev. B* **100** (2019), no. 12, article ID 125108.
[238] M. Yan *et al.*, "On-chip valley topological materials for elastic wave manipulation", *Nat. Mater.* **17** (2018), no. 11, p. 993.
[239] F. Gao *et al.*, "Topologically protected refraction of robust kink states in valley photonic crystals", *Nat. Phys.* **14** (2018), no. 2, p. 140.
[240] Z. Wang *et al.*, "Guiding robust valley-dependent edge states by surface acoustic waves", *J. Appl. Phys.* **125** (2019), no. 4, article ID 044502.
[241] X.-D. Chen *et al.*, "Valley-contrasting physics in all-dielectric photonic crystals: orbital angular momentum and topological propagation", *Phys. Rev. B* **96** (2017), no. 2, article ID 020202.
[242] X. Liu, Q. Guo, J. Yang, "Tunable acoustic valley edge states in a flow-free resonator system", *Appl. Phys. Lett.* **115** (2019), no. 7, article ID 074102.
[243] H. Jiang *et al.*, "Acoustic valley edge states in a graphene-like system with sub-wavelength resonator", *J. Acoust. Soc. Am.* **146** (2019), no. 1, p. 736-741.
[244] X. Wen *et al.*, "Acoustic Dirac degeneracy and topological phase transitions realized by rotating scatterers", *J. Appl. Phys.* **123** (2018), no. 9, article ID 091703.
[245] D. Jia *et al.*, "Acoustic topological insulator by honeycomb sonic crystals with direct and indirect band gaps", *New J. Phys.* **20** (2018), no. 9, article ID 093027.
[246] J. Noh *et al.*, "Observation of photonic topological valley Hall edge states", *Phys. Rev. Lett.* **120** (2018), no. 6, article ID 063902.
[247] J. Lu *et al.*, "Observation of topological valley transport of sound in sonic crystals", *Nat. Phys.* **13** (2017), no. 4, p. 369.
[248] N. Laforge *et al.*, "Observation of topological gravity-capillary waves in a water wave crystal", *New J. Phys.* **21** (2019), no. 8, article ID 083031.
[249] J. K. Asbóth, B. Tarasinski, P. Delplace, "Chiral symmetry and bulk-boundary correspondence in periodically driven one-dimensional systems", *Phys. Rev. B* **90** (2014), no. 12, article ID 125143.
[250] V. Dal Lago, M. Atala, L. E. F. Foa Torres, "Floquet topological transitions in a driven one-dimensional topological insulator", *Phys. Rev. A* **92** (2015), no. 2, article ID 023624.
[251] M. Fruchart, "Complex classes of periodically driven topological lattice systems", *Phys. Rev. B* **93** (2016), no. 11, article ID 115429.
[252] N. H. Lindner, G. Refael, V. Galitski, "Floquet topological insulator in semiconductor quantum wells", *Nat. Phys.* **7** (2011), no. 6, p. 490.
[253] L. He *et al.*, "Floquet Chern insulators of light", *Nat. Commun.* **10** (2019), no. 1, p. 1-6.
[254] L. J. Maczewsky *et al.*, "Observation of photonic anomalous Floquet topological insulators", *Nat. Commun.* **8** (2017), article ID 13756.
[255] X.-L. Lü, H. Xie, "Topological phases and pumps in the Su–Schrieffer–Heeger model periodically modulated in time", *J. Phys.: Condens. Matter* **31** (2019), no. 49, article ID 495401.
[256] Q. Cheng *et al.*, "Observation of anomalous π modes in photonic Floquet engineering", *Phys. Rev. Lett.* **122** (2019), no. 17, article ID 173901.
[257] X. Liu, Q. Guo, J. Yang, "Miniaturization of Floquet topological insulators for airborne acoustics by thermal control", *Appl. Phys. Lett.* **114** (2019), no. 5, article ID 054102.
[258] L. He *et al.*, "Floquet Chern Insulators of Light", *preprint*, arXiv:1902.08560 (2019).
[259] C. M. Dai, W. Wang, X. X. Yi, "Photonic Floquet topological insulators with fluctuations and disorders", *Phys. Rev. A* **99** (2019), no. 3, article ID 033844.
[260] Y. Long, J. Ren, "Floquet topological acoustic resonators and acoustic Thouless pumping", *J. Acoust. Soc. Am.* **146** (2019), no. 1, p. 742-747.

[261] Y.-G. Peng, Z.-G. Geng, X.-F. Zhu, "Topologically protected bound states in one-dimensional Floquet acoustic waveguide systems", *J. Appl. Phys.* **123** (2018), no. 9, article ID 091716.

[262] Y.-G. Peng *et al.*, "Low-loss and broadband anomalous Floquet topological insulator for airborne sound", *Appl. Phys. Lett.* **110** (2017), no. 17, article ID 173505.

[263] W. Zhang, X. Chen, F. Ye, "Plasmonic topological insulators for topological nanophotonics", *Opt. Lett.* **42** (2017), no. 20, p. 4063-4066.

[264] S. Mukherjee *et al.*, "Experimental observation of anomalous topological edge modes in a slowly driven photonic lattice", *Nat. Commun.* **8** (2017), article ID 13918.

[265] M. Oudich *et al.*, "Space-time phononic crystals with anomalous topological edge states", *Phys. Rev. Res.* **1** (2019), no. 3, article ID 033069.

[266] Y. Zhang *et al.*, "Photonic Floquet topological insulators in atomic ensembles", *Laser Photonics Rev.* **9** (2015), no. 3, p. 331-338.

[267] H. Chen *et al.*, "Mechanical quantum Hall effect in time-modulated elastic materials", *Phys. Rev. Appl.* **11** (2019), no. 4, article ID 044029.

[268] M. C. Rechtsman *et al.*, "Photonic Floquet topological insulators", *Nature* **496** (2013), no. 7444, p. 196.

[269] R. Fleury, A. B. Khanikaev, A. Alu, "Floquet topological insulators for sound", *Nat. Commun.* **7** (2016), article ID 11744.

[270] M. Pasek, Y. D. Chong, "Network models of photonic Floquet topological insulators", *Phys. Rev. B* **89** (2014), no. 7, article ID 075113.

[271] P. Delplace, M. Fruchart, C. Tauber, "Phase rotation symmetry and the topology of oriented scattering networks", *Phys. Rev. B* **95** (2017), no. 20, article ID 205413.

[272] M. S. Rudner *et al.*, "Anomalous edge states and the bulk-edge correspondence for periodically driven two-dimensional systems", *Phys. Rev. X* **3** (2013), no. 3, article ID 031005.

[273] W. Hu *et al.*, "Measurement of a topological edge invariant in a microwave network", *Phys. Rev. X* **5** (2015), no. 1, article ID 011012.

[274] Y.-G. Peng *et al.*, "Experimental demonstration of anomalous Floquet topological insulator for sound", *Nat. Commun.* **7** (2016), article ID 13368.

[275] D. Leykam, M. C. Rechtsman, Y. D. Chong, "Anomalous topological phases and unpaired Dirac cones in photonic Floquet topological insulators", *Phys. Rev. Lett.* **117** (2016), no. 1, article ID 013902.

[276] M. Neupane *et al.*, "Observation of topological nodal fermion semimetal phase in ZrSiS", *Phys. Rev. B* **93** (2016), no. 20, article ID 201104.

[277] L. Xia *et al.*, "Observation of hourglass nodal lines in photonics", *Phys. Rev. Lett.* **122** (2019), no. 10, article ID 103903.

[278] M. Kim *et al.*, "Topologically nontrivial photonic nodal surface in a photonic metamaterial", *Phys. Rev. B* **99** (2019), no. 23, article ID 235423.

[279] W. Deng *et al.*, "Nodal rings and drumhead surface states in phononic crystals", *Nat. Commun.* **10** (2019), no. 1, p. 1769.

[280] H. Weng *et al.*, "Topological node-line semimetal in three-dimensional graphene networks", *Phys. Rev. B* **92** (2015), no. 4, article ID 045108.

[281] W. Gao *et al.*, "Experimental observation of photonic nodal line degeneracies in metacrystals", *Nat. Commun.* **9** (2018), no. 1, p. 950.

[282] H. C. Po, Y. Bahri, A. Vishwanath, "Phonon analog of topological nodal semimetals", *Phys. Rev. B* **93** (2016), no. 20, article ID 205158.

[283] L. Lu *et al.*, "Experimental observation of Weyl points", *Science* **349** (2015), no. 6248, p. 622-624.

[284] S.-Y. Xu *et al.*, "Discovery of a Weyl fermion semimetal and topological Fermi arcs", *Science* **349** (2015), no. 6248, p. 613-617.

[285] Y. Liu, Y. Xu, W. Duan, "Three-dimensional topological states of phonons with tunable pseudospin physics", *Research* **2019** (2019), article ID 5173580.

[286] M. Kim *et al.*, "Extremely broadband topological surface states in a photonic topological metamaterial", *Adv. Opt. Mater.* **7** (2019), article ID 1900900.

[287] L. Wang, S.-K. Jian, H. Yao, "Topological photonic crystal with equifrequency Weyl points", *Phys. Rev. A* **93** (2016), no. 6, article ID 061801.

[288] W. Ye *et al.*, "Photonic Hall effect and helical Zitterbewegung in a synthetic Weyl system", *Light: Sci. Appl.* **8** (2019), no. 1, p. 49.

[289] Y. Lu *et al.*, "Probing the Berry curvature and Fermi arcs of a Weyl circuit", *Phys. Rev. B* **99** (2019), no. 2, article ID 020302.

[290] H. Zhou *et al.*, "Observation of bulk Fermi arc and polarization half charge from paired exceptional points", *Science* **359** (2018), no. 6379, p. 1009-1012.

[291] A. A. Zyuzin, V. A. Zyuzin, "Chiral electromagnetic waves in Weyl semimetals", *Phys. Rev. B* **92** (2015), no. 11, article ID 115310.

[292] E. Goi *et al.*, "Observation of type I photonic Weyl points in optical frequencies", *Laser Photonics Rev.* **12** (2018), no. 2, article ID 1700271.

[293] Z. Yang, B. Zhang, "Acoustic type-II Weyl nodes from stacking dimerized chains", *Phys. Rev. Lett.* **117** (2016), no. 22, article ID 224301.

[294] B. Xie *et al.*, "Experimental realization of type-II Weyl points and Fermi arcs in phononic crystal", *Phys. Rev. Lett.* **122** (2019), no. 10, article ID 104302.

[295] X. Shi *et al.*, "Elastic Weyl points and surface arc states in three-dimensional structures", *Phys. Rev. Appl.* **12** (2019), no. 2, article ID 024058.

[296] Z. Song, X. Dai, "Hear the sound of Weyl fermions", *Phys. Rev. X* **9** (2019), no. 2, article ID 021053.

[297] Z. Yin *et al.*, "Tunable THz generalized Weyl points", *Opt. Express* **27** (2019), no. 2, p. 512-522.

[298] H. Ge *et al.*, "Experimental observation of acoustic weyl points and topological surface states", *Phys. Rev. Appl.* **10** (2018), no. 1, article ID 014017.

[299] M. Fruchart *et al.*, "Soft self-assembly of Weyl materials for light and sound", *Proc. Natl Acad. Sci. USA* **115** (2018), no. 16, p. E3655-E3664.

[300] D. Liu, J. Shi, "Circular phonon dichroism in Weyl semimetals", *Phys. Rev. Lett.* **119** (2017), no. 7, article ID 075301.

[301] T. Zhang *et al.*, "Double-weyl phonons in transition-metal monosilicides", *Phys. Rev. Lett.* **120** (2018), no. 1, article ID 016401.

[302] W. Gao *et al.*, "Photonic Weyl degeneracies in magnetized plasma", *Nat. Commun.* **7** (2016), article ID 12435.

[303] W.-J. Chen, M. Xiao, C. T. Chan, "Photonic crystals possessing multiple Weyl points and the experimental observation of robust surface states", *Nat. Commun.* **7** (2016), article ID 13038.

[304] S. M. Young *et al.*, "Dirac semimetal in three dimensions", *Phys. Rev. Lett.* **108** (2012), no. 14, article ID 140405.

[305] L. Lu *et al.*, "Symmetry-protected topological photonic crystal in three dimensions", *Nat. Phys.* **12** (2016), no. 4, p. 337.

[306] Y. Yang *et al.*, "Realization of a three-dimensional photonic topological insulator", *Nature* **565** (2019), no. 7741, p. 622.

[307] H.-X. Wang *et al.*, "Type-ii dirac photons", *NPJ Quantum Mater.* **2** (2017), no. 1, p. 54.

[308] Q. Guo *et al.*, "Three dimensional photonic Dirac points in metamaterials", *Phys. Rev. Lett.* **119** (2017), no. 21, article ID 213901.

[309] J. Y. Lin *et al.*, "Line nodes, Dirac points, and Lifshitz transition in two-dimensional nonsymmorphic photonic crystals", *Phys. Rev. B* **96** (2017), no. 7, article ID 075438.

[310] S. Borisenko *et al.*, "Experimental realization of a three-dimensional Dirac semimetal", *Phys. Rev. Lett.* **113** (2014), no. 2, article ID 027603.

[311] S. M. Young, C. L. Kane, "Dirac semimetals in two dimensions", *Phys. Rev. Lett.* **115** (2015), no. 12, article ID 126803.

[312] L. Lu *et al.*, "Weyl points and line nodes in gyroid photonic crystals", *Nat. Photonics* **7** (2013), no. 4, p. 294.

[313] M. Xiao *et al.*, "Synthetic gauge flux and Weyl points in acoustic systems", *Nat. Phys.* **11** (2015), no. 11, p. 920.

[314] F. Li *et al.*, "Weyl points and Fermi arcs in a chiral phononic crystal", *Nat. Phys.* **14** (2018), no. 1, p. 30.

[315] Q. Lin *et al.*, "Photonic Weyl point in a two-dimensional resonator lattice with a synthetic frequency dimension", *Nat. Commun.* **7** (2016), article ID 13731.

[316] M. G. Silveirinha, "Bulk-edge correspondence for topological photonic continua", *Phys. Rev. B* **94** (2016), no. 20, article ID 205105.

[317] S. Afzal, V. Van, "Topological phases and the bulk-edge correspondence in 2D photonic microring resonator lattices", *Opt. Express* **26** (2018), no. 11, p. 14567-14577.

[318] R.-J. Slager *et al.*, "Impurity-bound states and Green's function zeros as local signatures of topology", *Phys. Rev. B* **92** (2015), no. 8, article ID 085126.

[319] A. E. Hassan *et al.*, "Corner states of light in photonic waveguides", *Nat. Photon.* **13** (2019), no. 10, p. 697-700.

[320] B.-Y. Xie *et al.*, "Visualization of higher-order topological insulating phases in two-dimensional dielectric photonic crystals", *Phys. Rev. Lett.* **122** (2019), no. 23, article ID 233903.

[321] F. Liu, H.-Y. Deng, K. Wakabayashi, "Helical topological edge states in a quadrupole phase", *Phys. Rev. Lett.* **122** (2019), no. 8, article ID 086804.

[322] X. Zhang *et al.*, "Acoustic hierarchical topological insulators", *preprint*, arXiv:1811.05514 (2018).

[323] S.-y. Huo *et al.*, "Edge states and corner modes in second-order topological phononic crystal plates", *preprint*, arXiv:1905.09731 (2019).

[324] T. Mizoguchi, H. Araki, Y. Hatsugai, "Higher-order topological phase in a honeycomb-lattice model with anti-Kekulé distortion", *J. Phys. Soc. Japan* **88** (2019), no. 10, article ID 104703.

[325] H. Fan *et al.*, "Elastic higher-order topological insulator with topologically protected corner states", *Phys. Rev. Lett.* **122** (2019), no. 20, article ID 204301.

[326] W. A. Benalcazar, B. A. Bernevig, T. L. Hughes, "Quantized electric multipole insulators", *Science* **357** (2017), no. 6346, p. 61-66.

[327] S. Imhof *et al.*, "Topolectrical-circuit realization of topological corner modes", *Nat. Phys.* **14** (2018), no. 9, p. 925.

[328] C. W. Peterson *et al.*, "A quantized microwave quadrupole insulator with topologically protected corner states", *Nature* **555** (2018), no. 7696, p. 346.
[329] H. Xue *et al.*, "Acoustic higher-order topological insulator on a kagome lattice", *Nat. Mater.* **18** (2019), no. 2, p. 108.
[330] X. Ni *et al.*, "Observation of higher-order topological acoustic states protected by generalized chiral symmetry", *Nat. Mater.* **18** (2019), no. 2, p. 113.
[331] M. Serra-Garcia *et al.*, "Observation of a phononic quadrupole topological insulator", *Nature* **555** (2018), no. 7696, p. 342.
[332] X. Zhang *et al.*, "Second-order topology and multidimensional topological transitions in sonic crystals", *Nat. Phys.* **15** (2019), p. 582-588.
[333] S. A. A. Ghorashi *et al.*, "Second-order Dirac superconductors and magnetic field induced Majorana hinge modes", *Phys. Rev. B* **100** (2019), no. 2, article ID 020509.
[334] Y. Ota *et al.*, "Photonic crystal nanocavity based on a topological corner state", *Optica* **6** (2019), no. 6, p. 786-789.
[335] Y. Chen, X. Lu, H. Chen, "Effect of truncation on photonic corner states in a Kagome lattice", *Opt. Lett.* **44** (2019), no. 17, p. 4251-4254.
[336] B. Liu *et al.*, "Two-dimensional quadrupole topological insulator in γ-graphyne", *Nano Lett.* **19** (2019), no. 9, p. 6492-6497.
[337] L. Zhang *et al.*, "Higher-order photonic topological states in surface-wave photonic crystals", *preprint*, arXiv:1901.07154 (2019).
[338] S. N. Kempkes *et al.*, "Robust zero-energy modes in an electronic higher-order topological insulator", *Nat. Mater.* **18** (2019), p. 1292-1297.
[339] X.-D. Chen *et al.*, "Direct observation of corner states in second-order topological photonic crystal slabs", *Phys. Rev. Lett.* **122** (2019), no. 23, article ID 233902.
[340] Y. Volpez, D. Loss, J. Klinovaja, "Second-order topological superconductivity in π-junction rashba layers", *Phys. Rev. Lett.* **122** (2019), no. 12, article ID 126402.
[341] S.-B. Zhang, B. Trauzettel, "Detection of second-order topological superconductors by Josephson junctions", *Phys. Rev. Res.* **2** (2020), no. 1, article ID 012018.
[342] X.-L. Sheng *et al.*, "Two-dimensional second-order topological insulator in graphdiyne", *preprint*, arXiv:1904.09985 (2019).
[343] A. Agarwala, V. Juricic, B. Roy, "Higher Order Topological Insulators in Amorphous Solids", *preprint*, arXiv:1902.00507 (2019).
[344] S. Mittal *et al.*, "Photonic quadrupole topological phases", *Nat. Photonics* **13** (2019), p. 692-696.
[345] M. Weiner *et al.*, "Demonstration of a 3rd order hierarchy of higher order topological states in a three-dimensional acoustic metamaterial", *preprint*, arXiv:1903.00428 (2019).
[346] H. Xue *et al.*, "Realization of an acoustic third-order topological insulator", *Phys. Rev. Lett.* **122** (2019), no. 24, article ID 244301.
[347] X. Zhou *et al.*, "Optical isolation with nonlinear topological photonics", *New J. Phys.* **19** (2017), no. 9, article ID 095002.
[348] D. Leykam, Y. D. Chong, "Edge solitons in nonlinear-photonic topological insulators", *Phys. Rev. Lett.* **117** (2016), no. 14, article ID 143901.
[349] D. R. Gulevich *et al.*, "Exploring nonlinear topological states of matter with exciton-polaritons: edge solitons in kagome lattice", *Sci. Rep.* **7** (2017), no. 1, p. 1780.
[350] R. K. Pal *et al.*, "Amplitude-dependent topological edge states in nonlinear phononic lattices", *Phys. Rev. E* **97** (2018), no. 3, article ID 032209.
[351] B. G.-g. Chen, N. Upadhyaya, V. Vitelli, "Nonlinear conduction via solitons in a topological mechanical insulator", *Proc. Natl Acad. Sci. USA* **111** (2014), no. 36, p. 13004-13009.
[352] D. D. J. M. Snee, Y.-P. Ma, "Edge solitons in a nonlinear mechanical topological insulator", *Extreme Mech. Lett.* **76** (2019), article ID 100487.
[353] Y. Hadad, A. B. Khanikaev, A. Alu, "Self-induced topological transitions and edge states supported by nonlinear staggered potentials", *Phys. Rev. B* **93** (2016), no. 15, article ID 155112.
[354] Y. Hadad *et al.*, "Self-induced topological protection in nonlinear circuit arrays", *Nat. Electron.* **1** (2018), no. 3, p. 178.
[355] D. A. Dobrykh *et al.*, "Nonlinear control of electromagnetic topological edge states", *Phys. Rev. Lett.* **121** (2018), no. 16, article ID 163901.
[356] R. Chaunsali, T. Georgios, "Self-induced topological transition in phononic crystals by nonlinearity management", *Phys. Rev. B* **100** (2019), no. 1, article ID 014302.
[357] F. Zangeneh-Nejad, R. Fleury, "Nonlinear second-order topological insulators", *Phys. Rev. Lett.* **123** (2019), article ID 053902.
[358] A. Blanco-Redondo *et al.*, "Topological optical waveguiding in silicon and the transition between topological and trivial defect states", *Phys. Rev. Lett.* **116** (2016), no. 16, article ID 163901.

[359] L. Shen *et al.*, "Backscattering-immune one-way surface magnetoplasmons at terahertz frequencies", *Opt. Express* **23** (2015), no. 2, p. 950-962.
[360] H. Xu *et al.*, "Topological energy transfer in an optomechanical system with exceptional points", *Nature* **537** (2016), no. 7618, p. 80.
[361] Y.-X. Shen *et al.*, "Observation of low-loss broadband supermode propagation in coupled acoustic waveguide complex", *Sci. Rep.* **7** (2017), article ID 45603.
[362] Q. Wei *et al.*, "Experimental demonstration of topologically protected efficient sound propagation in an acoustic waveguide network", *Phys. Rev. B* **95** (2017), no. 9, article ID 094305.
[363] T. Jiang *et al.*, "Experimental demonstration of angular momentum-dependent topological transport using a transmission line network", *Nat. Commun.* **10** (2019), no. 1, p. 434.
[364] Y. Guo, T. Dekorsy, M. Hettich, "Topological guiding of elastic waves in phononic metamaterials based on 2D pentamode structures", *Sci. Rep.* **7** (2017), no. 1, article ID 18043.
[365] O. Oltulu *et al.*, "Topological insulator based locally resonant phononic crystals: wave propagation and acoustic band gaps", *Ferroelectrics* **499** (2016), no. 1, p. 123-129.
[366] R. Deshmukh *et al.*, "Long-range resonant energy transfer using optical topological transitions in metamaterials", *ACS Photonics* **5** (2018), no. 7, p. 2737-2741.
[367] C.-C. Chien *et al.*, "Topological quantization of energy transport in micromechanical and nanomechanical lattices", *Phys. Rev. B* **97** (2018), no. 12, article ID 125425.
[368] V. Peano *et al.*, "Topological phase transitions and chiral inelastic transport induced by the squeezing of light", *Nat. Commun.* **7** (2016), article ID 10779.
[369] S. A. H. Gangaraj, A. Nemilentsau, G. W. Hanson, "The effects of three-dimensional defects on one-way surface plasmon propagation for photonic topological insulators comprised of continuum media", *Sci. Rep.* **6** (2016), article ID 30055.
[370] A. P. Slobozhanyuk *et al.*, "Subwavelength topological edge states in optically resonant dielectric structures", *Phys. Rev. Lett.* **114** (2015), no. 12, article ID 123901.
[371] C.-Y. Ji *et al.*, "Transport tuning of photonic topological edge states by optical cavities", *Phys. Rev. A* **99** (2019), no. 4, article ID 043801.
[372] W.-M. Deng *et al.*, "Vortex index identification and unidirectional propagation in Kagome photonic crystals", *Nanophotonics* **8** (2019), no. 5, p. 833-840.
[373] M. He, L. Zhang, H. Wang, "Two-dimensional photonic crystal with ring degeneracy and its topological protected edge states", *Sci. Rep.* **9** (2019), no. 1, p. 3815.
[374] P. Wang, L. Lu, K. Bertoldi, "Topological phononic crystals with one-way elastic edge waves", *Phys. Rev. Lett.* **115** (2015), no. 10, article ID 104302.
[375] H. Dai *et al.*, "Observation of topological edge states of acoustic metamaterials at subwavelength scale", *J. Phys. D: Appl. Phys.* **51** (2018), no. 17, article ID 175302.
[376] Y. Jin, D. Torrent, B. Djafari-Rouhani, "Robustness of conventional and topologically protected edge states in phononic crystal plates", *Phys. Rev. B* **98** (2018), no. 5, article ID 054307.
[377] I. Kim, S. Iwamoto, Y. Arakawa, "Topologically protected elastic waves in one-dimensional phononic crystals of continuous media", *Appl. Phys. Express* **11** (2017), no. 1, article ID 017201.
[378] H. Liu *et al.*, "Thermally tunable topological edge states for in-plane bulk waves in solid phononic crystals", *Ultrasonics* **94** (2019), p. 227-234.
[379] B. Xie *et al.*, "Multiband asymmetric transmission of airborne sound by coded metasurfaces", *Phys. Rev. Appl.* **7** (2017), no. 2, article ID 024010.
[380] Z.-G. Chen *et al.*, "Multiple topological phase transitions in a gyromagnetic photonic crystal", *Phys. Rev. A* **95** (2017), no. 4, article ID 043827.
[381] S. A. Mann, D. L. Sounas, A. Alù, "Broadband delay lines and nonreciprocal resonances in unidirectional waveguides", *Phys. Rev. B* **100** (2019), article ID 020303.
[382] Y. V. Kartashov, D. V. Skryabin, "Two-dimensional topological polariton laser", *Phys. Rev. Lett.* **122** (2019), no. 8, article ID 083902.
[383] B. Bahari *et al.*, "Nonreciprocal lasing in topological cavities of arbitrary geometries", *Science* **358** (2017), no. 6363, p. 636-640.
[384] X.-C. Sun, X. Hu, "Topological ring-cavity laser formed by honeycomb photonic crystals", *preprint*, arXiv:1906.02464 (2019).
[385] C. Han *et al.*, "Lasing at topological edge states in a photonic crystal L3 nanocavity dimer array", *Light: Sci. Appl.* **8** (2019), no. 1, p. 40.
[386] J.-L. Xu *et al.*, "Ultrasensitive nonlinear absorption response of large-size topological insulator and application in low-threshold bulk pulsed lasers", *Sci. Rep.* **5** (2015), article ID 14856.
[387] H. Zhao *et al.*, "Topological hybrid silicon microlasers", *Nat. Commun.* **9** (2018), no. 1, p. 981.

[388] L. Pilozzi, C. Conti, "Topological cascade laser for frequency comb generation in PT-symmetric structures", *Opt. Lett.* **42** (2017), no. 24, p. 5174-5177.

[389] G. Harari *et al.*, "Topological insulator laser: theory", *Science* **359** (2018), no. 6381, article ID eaar4003.

[390] M. Hafezi *et al.*, "Robust optical delay lines with topological protection", *Nat. Phys.* **7** (2011), no. 11, p. 907.

[391] M. Hafezi *et al.*, "Imaging topological edge states in silicon photonics", *Nat. Photon.* **7** (2013), no. 12, p. 1001.

[392] M. A. Bandres *et al.*, "Topological insulator laser: experiments", *Science* **359** (2018), no. 6381, article ID eaar4005.

[393] F. Zangeneh-Nejad, R. Fleury, "Topological fano resonances", *Phys. Rev. Lett.* **122** (2019), no. 1, article ID 014301.

[394] A. Silva *et al.*, "Performing mathematical operations with metamaterials", *Science* **343** (2014), no. 6167, p. 160-163.

[395] A. Youssefi *et al.*, "Analog computing by Brewster effect", *Opt. Lett.* **41** (2016), no. 15, p. 3467-3470.

[396] F. Zangeneh-Nejad, R. Fleury, "Performing mathematical operations using high-index acoustic metamaterials", *New J. Phys.* **20** (2018), no. 7, article ID 073001.

[397] N. M. Estakhri, B. Edwards, N. Engheta, "Inverse-designed metastructures that solve equations", *Science* **363** (2019), no. 6433, p. 1333-1338.

[398] F. Zangeneh-Nejad, A. Khavasi, B. Rejaei, "Analog optical computing by half-wavelength slabs", *Opt. Commun.* **407** (2018), p. 338-343.

[399] F. Zangeneh-Nejad, A. Khavasi, "Spatial integration by a dielectric slab and its planar graphene-based counterpart", *Opt. Lett.* **42** (2017), no. 10, p. 1954-1957.

[400] F. Zangeneh-Nejad, R. Fleury, "Topological analog signal processing", *Nat. Commun.* **10** (2019), no. 1, p. 2058.

[401] M. Ezawa, "Topological switch between second-order topological insulators and topological crystalline insulators", *Phys. Rev. Lett.* **121** (2018), no. 11, article ID 116801.

[402] R. Süsstrunk, P. Zimmermann, S. D. Huber, "Switchable topological phonon channels", *New J. Phys.* **19** (2017), no. 1, article ID 015013.

[403] Y. Fan *et al.*, "Magnetization switching through giant spin-orbit torque in a magnetically doped topological insulator heterostructure", *Nat. Mater.* **13** (2014), no. 7, p. 699.

[404] J. Han *et al.*, "Room-temperature spin-orbit torque switching induced by a topological insulator", *Phys. Rev. Lett.* **119** (2017), no. 7, article ID 077702.

[405] N. H. D. Khang, Y. Ueda, P. N. Hai, "A conductive topological insulator with large spin Hall effect for ultralow power spin-orbit torque switching", *Nat. Mater.* **17** (2018), p. 808-813.

[406] J. Lee *et al.*, "All-fiberized, passively Q-switched 1.06 μm laser using a bulk-structured Bi_2Te_3 topological insulator", *J. Opt.* **16** (2014), no. 8, article ID 085203.

[407] Y. Chen *et al.*, "Large energy, wavelength widely tunable, topological insulator Q-switched erbium-doped fiber laser", *IEEE J. Sel. Top. Quantum Electron.* **20** (2013), no. 5, p. 315-322.

[408] H. Yu *et al.*, "Topological insulator as an optical modulator for pulsed solid-state lasers", *Laser Photonics Rev.* **7** (2013), no. 6, p. L77-L83.

[409] X. B. Wang *et al.*, "Topological-insulator-based terahertz modulator", *Sci. Rep.* **7** (2017), no. 1, article ID 13486.

[410] X. Xiao *et al.*, "All-electric spin modulator based on a two-dimensional topological insulator", *Appl. Phys. Lett.* **108** (2016), no. 3, article ID 032403.

[411] F. Hassler, A. R. Akhmerov, C. W. J. Beenakker, "Flat-lens focusing of electrons on the surface of a topological insulator", *Phys. Rev. B* **82** (2010), no. 12, article ID 125423.

[412] H. He *et al.*, "Topological negative refraction of surface acoustic waves in a Weyl phononic crystal", *Nature* **560** (2018), no. 7716, p. 61.

[413] T. Fujita, M. B. A. Jalil, S. G. Tan, "Topological insulator cell for memory and magnetic sensor applications", *Appl. Phys. Express* **4** (2011), no. 9, article ID 094201.

[414] L. Ye *et al.*, "Observation of acoustic valley vortex states and valley-chirality locked beam splitting", *Phys. Rev. B* **95** (2017), no. 17, article ID 174106.

[415] P. Qiu *et al.*, "Plasmonic valley chiral states in graphene based plasmonic crystals", *J. Phys. D: Appl. Phys.* **52** (2018), no. 1, article ID 015102.

[416] M. P. Makwana, R. Craster, S. Guenneau, "Novel topological beam-splitting in photonic crystals", *preprint*, arXiv:1902.00072 (2019).

[417] D. G. Rothe, E. M. Hankiewicz, "Tunable polarization in a beam splitter based on two-dimensional topological insulators", *Phys. Rev. B* **89** (2014), no. 3, article ID 035418.

[418] M. Makwana, R. Craster, S. Guenneau, "Topological beam-splitting in photonic crystals", *Opt. Express* **27** (2019), no. 11, p. 16088-16102.

[419] J. Lee *et al.*, "Passively Q-Switched 1.89-μm fiber laser using a bulk-structured Bi_2Te_3 topological insulator", *IEEE J. Sel. Top. Quantum Electron.* **21** (2014), no. 1, p. 31-36.

[420] H. Liu *et al.*, "Femtosecond pulse generation from a topological insulator mode-locked fiber laser", *Opt. Express* **22** (2014), no. 6, p. 6868-6873.

[421] Z.-C. Luo *et al.*, "2 GHz passively harmonic mode-locked fiber laser by a microfiber-based topological insulator saturable absorber", *Opt. Lett.* **38** (2013), no. 24, p. 5212-5215.

[422] M. Liu *et al.*, "Dual-wavelength harmonically mode-locked fiber laser with topological insulator saturable absorber", *IEEE Photonics Technol. Lett.* **26** (2014), no. 10, p. 983-986.

[423] P. Yan, R. Lin, H. Chen, H. Zhang, A. Liu, H. Yang, S. Ruan, "Topological insulator solution filled in photonic crystal fiber for passive mode-locked fiber laser", *IEEE Photonics Technol. Lett.* **27** (2014), no. 3, p. 264-267.

[424] F. Bernard *et al.*, "Towards mode-locked fiber laser using topological insulators", in *Nonlinear Photonics*, Optical Society of America, 2012.

[425] Z.-G. Geng *et al.*, "Acoustic delay-line filters based on largely distorted topological insulators", *Appl. Phys. Lett.* **113** (2018), no. 3, article ID 033503.

[426] Z. Zhang *et al.*, "Topological acoustic delay line", *Phys. Rev. Appl.* **9** (2018), no. 3, article ID 034032.

[427] K. Lai *et al.*, "Experimental realization of a reflections-free compact delay line based on a photonic topological insulator", *Sci. Rep.* **6** (2016), article ID 28453.

[428] Y. Wu *et al.*, "Applications of topological photonics in integrated photonic devices", *Adv. Optical Mater.* **5** (2017), no. 18, article ID 1700357.

[429] Y. Yang *et al.*, "Terahertz topological photonics for on-chip communication", *preprint*, arXiv:1904.04213 (2019).

[430] Z.-G. Chen *et al.*, "Acoustic frequency filter based on anisotropic topological phononic crystals", *Sci. Rep.* **7** (2017), no. 1, article ID 15005.

[431] F. Nathan, I. Martin, G. Refael, "Topological frequency conversion in a driven dissipative quantum cavity", *Phys. Rev. B* **99** (2019), no. 9, article ID 094311.

[432] Y. Wang *et al.*, "Topologically enhanced harmonic generation in a nonlinear transmission line metamaterial", *Nat. Commun.* **10** (2019), no. 1, p. 1102.

[433] C. Jürß, D. Bauer, "High-harmonic generation in Su–Schrieffer–Heeger chains", *Phys. Rev. B* **99** (2019), no. 19, article ID 195428.

[434] R. Ilan, F. De Juan, J. E. Moore, "Spin-based Mach-Zehnder interferometry in topological insulator p–n junctions", *Phys. Rev. Lett.* **115** (2015), no. 9, article ID 096802.

[435] V. Peano *et al.*, "Topological quantum fluctuations and traveling wave amplifiers", *Phys. Rev. X* **6** (2016), no. 4, article ID 041026.

[436] D. Malz, J. Knolle, A. Nunnenkamp, "Topological magnon amplification", *Nat. Commun.* **10** (2019), no. 1, p. 1-7.

[437] D. Leykam *et al.*, "Edge modes, degeneracies, and topological numbers in non-Hermitian systems", *Phys. Rev. Lett.* **118** (2017), no. 4, article ID 040401.

[438] K. Esaki *et al.*, "Edge states and topological phases in non-Hermitian systems", *Phys. Rev. B* **84** (2011), no. 20, article ID 205128.

[439] H. Zhao *et al.*, "Non-Hermitian topological light steering", *Science* **365** (2019), no. 6458, p. 1163-1166.

[440] M. S. Rudner, L. S. Levitov, "Topological transition in a non-hermitian quantum walk", *Phys. Rev. Lett.* **102** (2009), no. 6, article ID 065703.

[441] S. Longhi, D. Gatti, G. D. Valle, "Robust light transport in non-Hermitian photonic lattices", *Sci. Rep.* **5** (2015), article ID 13376.

[442] L. Li, C. H. Lee, J. Gong, "Geometric characterization of non-Hermitian topological systems through the singularity ring in pseudospin vector space", *Phys. Rev. B* **100** (2019), no. 7, article ID 075403.

[443] B. Midya, H. Zhao, L. Feng, "Non-Hermitian photonics promises exceptional topology of light", *Nat. Commun.* **9** (2018), no. 1, p. 2674.

[444] K. Y. Bliokh *et al.*, "Topological non-Hermitian origin of surface Maxwell waves", *Nat. Commun.* **10** (2019), no. 1, p. 580.

[445] A. Cerjan *et al.*, "Experimental realization of a Weyl exceptional ring", *Nat. Photon.* **13** (2019), p. 623-628.

[446] S. Malzard, C. Poli, H. Schomerus, "Topologically protected defect states in open photonic systems with non-Hermitian charge-conjugation and parity-time symmetry", *Phys. Rev. Lett.* **115** (2015), no. 20, article ID 200402.

[447] E. Edvardsson, F. K. Kunst, E. J. Bergholtz, "Non-Hermitian extensions of higher-order topological phases and their biorthogonal bulk-boundary correspondence", *Phys. Rev. B* **99** (2019), no. 8, article ID 081302.

[448] R. Chen *et al.*, "Finite-size effects in non-Hermitian topological systems", *Phys. Rev. B* **99** (2019), no. 15, article ID 155431.

[449] L. Xiao *et al.*, "Observation of topological edge states in parity-time-symmetric quantum walks", *Nat. Phys.* **13** (2017), no. 11, p. 1117.

[450] C. Sheng *et al.*, "Definite photon deflections of topological defects in metasurfaces and symmetry-breaking phase transitions with material loss", *Nat. Commun.* **9** (2018), no. 1, p. 4271.

[451] Ş. K. Özdemir *et al.*, "Parity-time symmetry and exceptional points in photonics", *Nat. Mater.* **18** (2019), p. 783-798.

[452] H. Shen, B. Zhen, L. Fu, "Topological band theory for non-Hermitian Hamiltonians", *Phys. Rev. Lett.* **120** (2018), no. 14, article ID 146402.

[453] Z. Gong *et al.*, "Topological phases of non-Hermitian systems", *Phys. Rev. X* **8** (2018), no. 3, article ID 031079.

[454] Y. Li *et al.*, "Waveguide metatronics: lumped circuitry based on structural dispersion", *Sci. Adv.* **2** (2016), no. 6, p. e1501790.

[455] H. M. Price *et al.*, "Four-dimensional quantum Hall effect with ultracold atoms", *Phys. Rev. Lett.* **115** (2015), no. 19, article ID 195303.
[456] M. Fremling *et al.*, "A Chern insulator in ln(8)/ln(3) dimensions", *preprint*, arXiv:1906.07387 (2019).
[457] Y. E. Kraus, Z. Ringel, O. Zilberberg, "Four-dimensional quantum Hall effect in a two-dimensional quasicrystal", *Phys. Rev. Lett.* **111** (2013), no. 22, article ID 226401.
[458] S.-C. Zhang, J. Hu, "A four-dimensional generalization of the quantum Hall effect", *Science* **294** (2001), no. 5543, p. 823-828.
[459] L. Yuan *et al.*, "Synthetic dimension in photonics", *Optica* **5** (2018), no. 11, p. 1396-1405.
[460] F. Mei *et al.*, "Topological insulator and particle pumping in a one-dimensional shaken optical lattice", *Phys. Rev. A* **90** (2014), no. 6, article ID 063638.
[461] E. Lustig *et al.*, "Photonic topological insulator in synthetic dimensions", *Nature* **567** (2019), no. 7748, p. 356.
[462] X.-W. Luo *et al.*, "Quantum simulation of 2D topological physics in a 1D array of optical cavities", *Nat. Commun.* **6** (2015), p. 7704.
[463] F. Mei *et al.*, "Simulating Z_2 topological insulators with cold atoms in a one-dimensional optical lattice", *Phys. Rev. A* **85** (2012), no. 1, article ID 013638.
[464] T. Ozawa, H. M. Price, "Topological quantum matter in synthetic dimensions", *Nat. Rev. Phys.* **1** (2019), p. 349-357.
[465] G. Salerno *et al.*, "Quantized Hall conductance of a single atomic wire: a proposal based on synthetic dimensions", *Phys. Rev. X* **9** (2019), no. 4, article ID 041001.
[466] C.-M. Jian, C. Xu, "Interacting topological insulators with synthetic dimensions", *Phys. Rev. X* **8** (2018), no. 4, article ID 041030.
[467] J. R. M. Silva *et al.*, "Phononic topological states in 1D quasicrystals", *J. Phys.: Condens. Matter* **31** (2019), article ID 505405.
[468] T. Ozawa *et al.*, "Synthetic dimensions in integrated photonics: from optical isolation to four-dimensional quantum Hall physics", *Phys. Rev. A* **93** (2016), no. 4, article ID 043827.
[469] D. J. Apigo *et al.*, "Observation of topological edge modes in a quasiperiodic acoustic waveguide", *Phys. Rev. Lett.* **122** (2019), no. 9, article ID 095501.
[470] Y. E. Kraus *et al.*, "Topological states and adiabatic pumping in quasicrystals", *Phys. Rev. Lett.* **109** (2012), no. 10, article ID 106402.
[471] M. Verbin *et al.*, "Observation of topological phase transitions in photonic quasicrystals", *Phys. Rev. Lett.* **110** (2013), no. 7, article ID 076403.
[472] Y. E. Kraus, O. Zilberberg, "Topological equivalence between the Fibonacci quasicrystal and the Harper model", *Phys. Rev. Lett.* **109** (2012), no. 11, article ID 116404.
[473] S. Ganeshan, K. Sun, S. D. Sarma, "Topological zero-energy modes in gapless commensurate Aubry–André–Harper models", *Phys. Rev. Lett.* **110** (2013), no. 18, article ID 180403.